Comparative genomic analysis of a metagenome-assembled genome reveals distinctive symbiotic traits in a Mucoromycotina fine root endophyte arbuscular mycorrhizal fungus

Joshua Cole[1*], Sébastien Raguideau[2], Payman Abbaszadeh-Dahaji[3,4], Sally Hilton[1], George Muscatt[1], Ryan M. Mushinski[1], R. Henrik Nilsson[5], Megan H. Ryan[3], Christopher Quince[2,6,7] and Gary D. Bending[1*]

[1]School of Life Sciences, University of Warwick, Coventry CV4 7AL, UK

[2]Earlham Institute, Norwich Research Park, Colney Lane, Norwich NR4 7UZ, UK

[3]UWA School of Agriculture and Environment, University of Western Australia, Crawley, WA, 6009, Australia

[4]Department of Soil Sciences, Faculty of Agricultural Science, Vali-e-Asr University of Rafsanjan, Rafsanjan, Iran

[5]University of Gothenburg, Department of Biological and Environmental Sciences, Gothenburg Global Biodiversity Centre, University of Gothenburg, Box 461, 405 30, Göteborg, Sweden

[6]Gut Microbes and Health, Quadram Institute, Norwich NR4 7UQ, UK

[7]School of Biological Sciences, University of East Anglia, Norwich NR4 7T, UK

*Corresponding authors: Joshua.M.Cole@warwick.ac.uk; gary.bending@warwick.ac.uk

ORCID

Joshua Cole - 0009-0004-1563-8469

Sébastien Raguideau - 0000-0001-8727-2604

Payman Abbaszadeh-Dahaji - 0000-0003-3055-4744

Sally Hilton - 0000-0002-3786-1096

George Muscatt - 0000-0002-9218-1210

Ryan M Mushinski - 0000-0003-3572-3500

R. Henrik Nilsson – 0000-0002-8052-0107

Megan H. Ryan – 0000-0003-0749-0199

Christopher Quince – 0000-0003-1884-8440

Gary D. Bending - 0000-0002-9740-5244

Summary

- Recent evidence shows that arbuscular mycorrhizal (AM) symbiosis is established by two distinct fungal groups, with the distinctive 'fine root endophyte' morphotype formed by fungi from the sub-phylum Mucoromycotina rather than the sub-phylum Glomeromycotina. While Mucoromycotina AM fungi are globally distributed, their genomic basis for the symbiosis or how this compares to other mycorrhizal symbionts is unknown.
- We used culture-independent metagenome sequencing to assemble and characterise the metagenome-assembled genome (MAG) of a putative fine root endophyte, which we show belonged to the family Planticonsortiaceae within the order Densosporales.
- The MAG shares key traits with Glomeromycotina fungi, which indicate obligate biotrophy, including absence of fatty acid and thiamine biosynthesis pathways, limited enzymatic abilities to degrade plant cell walls, and a high abundance of calcium transporters. In contrast to Glomeromycotina fungi, it exhibited a higher capacity for degradation of microbial cell walls, a complete cellulose degradation pathway, low abundances of copper, nitrate and ammonium transporters, and a complete pathway for vitamin B6 biosynthesis.
- These differences highlight the potential for contrasting interactions between Mucoromycotina and Glomeromycotina AM fungi with their host plant and the environment which could support niche differentiation and complementary ecological functions.

Introduction

Mutualistic symbioses with microbes are exhibited by the overwhelming majority of plant species (Begum, 2019) with mycorrhizas by far the most widespread and well-described association (Hawkins et al., 2023). While mycorrhizal symbioses have evolved multiple times across plant and fungal taxa, they share the common characteristic of the fungus trading nutrients assimilated from the soil, particularly phosphorus and nitrogen, in exchange for carbon from the plant (Luginbuehl & Oldroyd, 2017). Additionally, mycorrhizal associations can confer a range of secondary benefits to the plant host, including disease resistance and stress tolerance (Chen, 2018). Because of these profound impacts on plants, mycorrhizal associations are considered to be major determinants of ecosystem productivity and diversity and to play key roles in directing terrestrial biogeochemical cycling processes. There are four main groups of mycorrhizal associations: arbuscular (AM), ecto- (ECM), ericoid (ERM), and orchid (ORM) (Martin & van der Heijden, 2024) mycorrhizas, which are distinguished by a number of features including the specific plant and fungal taxa involved, the ecosystems they inhabit, the way in which the fungus colonises and grows within root tissues, and the functional traits of the fungi involved (Brundrett & Tedersoo, 2018).

As a function of time and niche specificity, mycorrhizal symbionts appear to have evolved along a saprotrophy to symbiosis continuum (Strullu-Derrien et al., 2018; Martin & van der Heijden, 2024). This directional transition from free-living saprotrophs to obligate symbionts is believed to be driven by the provision of carbohydrates and vitamins from plants in nutrient-poor environments and the subsequent evolutionary success of a symbiotic lifestyle. As a result, key genomic signatures associated with this transition can be identified across this continuum (Martin & van der Heijden, 2024). As fungal symbionts shift away from primarily saprotrophic lifestyles to mutualisms, their genomes typically possess a reduced repertoire of the enzymatic machinery involved in the degradation of soil organic matter (SOM) and plant cell walls (Martino et al., 2018; Gong et al., 2023; Martin & van der Heijden, 2024). The two youngest mycorrhizal symbioses, ERM and ORM, with origins c 75-90 and 112 mya, respectively, (Martino et al., 2018; Brundrett & Tedersoo, 2018) involve symbionts with genomic repertoires capable of simultaneously facilitating a saprotrophic and a symbiotic lifestyle. However, fungi forming the older AM (origin 450 mya, Brundrett & Tedersoo, 2018) and ECM symbioses (origin c 200 mya) possess a much more fine-tuned enzymatic toolkit, noted for a reduced suite of plant cell wall degrading enzymes (PCWDE)

along with the presence of specific genes involved in regulating nutrient transport and host plant signalling and metabolism (Martino et al., 2018; Martin & van der Heijden, 2024).

AM are considered the most common and widespread plant-microbe symbiosis on Earth (Read et al., 2000; Parniske, 2008; Spatafora et al., 2017), and their presence in fossil roots of the earliest land plants suggests that they were a significant factor in the evolution of land plants. Fungi forming AM have traditionally been placed into the Mucoromycota sub-phylum Glomeromycotina. These fungi are obligate symbionts; as fatty acid auxotrophs they depend on the exchange of plant derived fatty acids (Schüβler et al., 2007; Luginbuehl et al., 2017). As a result of long-term host dependence, arbuscular mycorrhizal fungi (AMF) present hallmark traits such as limited ability to break down cellulose, biosynthesise thiamine, or metabolise vitamin B6 derivatives. The genomic inability to express these hallmark traits represent Missing Glomeromycotan Core Genes (MGCGs) (Tang et al., 2016; Kobayashi et al., 2018; Rosling et al., 2024).

Until recently, all AMF were believed to belong to the Glomeromycotina (G-AMF) (Spatafora et al., 2017). It has long been recognised that there are two broad groups of arbuscular mycorrhiza based on morphology, with the ‘coarse endophyte’ G-AMF being the focus of the vast majority of research on the biology and ecology of AMF (Orchard et al., 2017b). Glomeromycotina comprises four orders, the Glomerales, Diversisporales, Paraglomerales, and Archaeosporales, which likely diversified when plants evolved onto land (Schüβle 2001; Chen et al., 2018; Tedersoo et al., 2018). The second morphological group of ‘fine root endophytes (FRE)’ arbuscular fungi are distinguished from coarse endophytes by their small spores, fan-shaped or palmate entry points, diverging thin hyphae (<2 µm diameter) which in intercellular spaces often form hyphal ropes, as well as intercalary and terminal 'vesicles”, approximately 5–10 µm in diameter (Thippayarugs et al. 1999; Orchard et al., 2017a, b; Walker et al. 2018). Interestingly, the arbuscules of FRE appear very similar in structure to those of coarse endophytes (Albornoz et al. 2020). Recent evidence has placed FRE within the sub-phylum Mucoromycotina (M-AMF) (Orchard et al., 2017b), indicating that AM symbioses may have evolved independently several times, as is the case for ectomycorrhizal symbioses (Miyauchi et al., 2020).

To date only one species of M-AMF, *Planticonsortium tenue*, has been described (Walker et al., 2018). However, similarly to G-AMF, root systems are colonised by diverse Mucoromycotina taxa, communities of which are typically comprised of a small number of abundant and common taxa and a high diversity of rare low-abundance taxa (Albornoz et al.,

2021, 2022; Seeliger et al., 2024). Furthermore, distinctive morphologies of FRE have been recognised (Thippayarugs et al., 1999) based on a variety of characteristics, including the roughness, diameter, and branching of hyphae and the size and shape of vesicles. While fungi within the Glomeromycotina are all assumed to be plant symbionts, fungi residing within the Mucoromycotina also include saprotrophs and putative ectomycorrhizal symbionts. Those Mucoromycotina sequences found associated with roots and rhizoids of vascular and non-vascular plants appear to have similar phylogenetic ranges and occur within clades alongside taxa with saprotrophic and putative ectomycorrhizal lifestyles (Desirò et al., 2017; Seeliger et al., 2024).

M-AMF have been detected across multiple continents, spanning a wide range of ecosystems, environmental conditions, and hosts, although in contrast to G-AMF they may be missing from tropical and sub-tropical biomes, and may be favoured by agricultural management practices (Orchard et al., 2017a; Albornoz et al., 2022). While the benefits of G-AMF to the host, particularly for phosphorus nutrition, are well documented, the functional significance of M-AMF within ecosystems is poorly understood (Orchard et al., 2017b; Hoysted et al., 2019; Albornoz et al., 2020). G-AMF and M-AMF typically co-occur and intermingle within root systems (Orchard et al., 2017a,b; Jeffery et al., 2018), but they appear to occupy distinct but overlapping ecological niches (e.g. Orchard et al. 2016), with their distribution at the landscape scale differentially determined by temperature, pH, and plant richness (Albornoz et al., 2022). Unlike G-AMF, nutrient availability was found to be an important determinant of M-AMF abundance, which increased with fertility (Albornoz et al., 2022). Furthermore, in contrast to G-AMF, experimental evidence suggests that M-AMF may provide the host with access to soil nitrogen, indicating a potential complementary functionality between the two arbuscular symbioses and an explanation for the parallel evolution of symbiotic traits (Hoysted et al., 2022; Howard et al., 2024).

Comparative genome analysis has emerged as a powerful tool to understand microbial evolution, function, and ecology. However, these approaches largely rely on the availability of cultured microbes or voucher specimens for whole genome sequencing (e.g. Martino et al., 2017; Miyauchi et al., 2020; Rosling et al., 2024). Importantly, culturing microbes can prove time-consuming and problematic as microbial populations have great complexity and many microbes have specific nutritional requirements which cannot be met in culture. This is particularly the case for obligate biotrophs such as symbionts which rely wholly or in-part on the host for their nutritional requirements (Tanaka et al., 2022). As obligate symbionts, G-

AMF require a host plant to complete their lifecycle. Despite this, pure cultures of G-AMF have been obtained using root organ cultures, and these have been used to produce inoculum for genome sequencing (Tisserant et al., 2013). The challenges in obtaining and maintaining root cultures have meant that direct genome sequencing of G-AMF cultures has been limited to date. Recently, asymbiotic mycelium and spore production of the G-AMF *Rhizophagus clarus* has been achieved by supplementing its growth medium with palmitoleic acid, and this could provide a boost to rates of culture-based sequencing (Tanaka et al., 2022). An alternative approach to obtain fungal genomes is sequencing of nuclei extracted from spores (Montoliu-Nerin et al., 2021), although most G-AMF taxa appear to sporulate infrequently, if at all (Öpik et al., 2014).

M-AMF are also putatively obligate symbionts, but because they have only recently been recognised as a distinct group of symbionts, culturing efforts lag behind those of G-AMF. Recently, monoxenic cultures of a Mucoromycotina fungus associated with the clubmoss *Lycopodiella inundata* have been obtained and shown to form FRE colonisation in a vascular plant (Hoystead et al., 2022). However, while genome sequencing and comparative genomic analysis of a number of saprotrophic and putative ectomycorrhizal Mucoromycotina has been achieved (Chang et al., 2019; Rosling et al., 2024), there is no understanding of the genome of M-AMF fungi and how their functional repertoire and mutualistic signatures compare to those of G-AMF, other mycorrhizal symbioses, and saprotrophic and putatively ectomycorrhizal Mucoromycotina. To further complicate the matter, initial comparative analysis of the sister clades indicate that some widely considered hallmark traits of mycorrhizal symbioses may instead represent ancestral markers as opposed to adaptation (Rosling et al., 2024).

Recently there has been great progress in the development of computational tools for the culture-independent assembly of ‘dark’ microbial genomes from metagenome sequencing datasets (Benoit et al., 2024). Such ‘Metagenome Assembled Genomes’ (MAGs) have been widely used to identify the metabolic capabilities and ecological roles of specific prokaryotes in diverse habitats (Yang et al., 2021). MAG construction of eukaryotic microbes is more challenging because of a range of issues including their large sizes, high genome heterozygosity, low abundance in metagenome datasets, and a lack of well annotated reference genomes for gene annotation (Peng et al., 2021; Setubal 2021). As a result, few studies have constructed eukaryotic MAGs from metagenomes, and these have typically been performed in low-diversity communities (e.g. West et al. 2018; Peng et al., 2021). A further

particular issue with analysis of plant symbionts *in situ* is their intimate association with plant tissue. This results in co-extraction of host DNA, increasing the sequencing depth required to assemble symbiont genomes.

The aim of the current work was to use culture-independent metagenome sequencing to assemble and characterise the genome of an FRE-forming M-AMF fungus for the first time and compare its genomic repertoire to glomeromycotan fungi and other fungal symbionts. Roots of *Trifolium subterraneum* were first enriched with FRE using a selective soil sieving technique. Root samples were used for metagenome sequencing, from which a MAG of the FRE was constructed. We compiled a database of 274 fungal genomes across the Ascomycota, Basidiomycota and Mucoromycota, and assigned these to G-AMF, ECM, ERM, OCM, saprotroph, pathogen, parasite, endophyte, lichenic, and mixed lifestyles. Comparative analysis showed that the MAG shares key distinctive characteristics with G-AMF. This includes overlaps in some MCGCs, presence of abundant calcium transporters, and an overall reduced set of plant cell wall degrading enzymes. However, we found a relatively high abundance of microbial cell wall degrading enzymes and evidence of complete cellulose degradation capability, as well as low numbers of nitrogen transporters, suggesting a distinctive niche relative to G-AMF and the other mycorrhizal lifestyles.

Materials and Methods

Soil collection and sample preparation

For the metagenome sequencing, plants with the root AMF community enriched in M-AMF were produced following the methods of Orchard et al. (2017a). In brief, soil was collected from the field studied by Orchard et al. (2016) and Orchard et al. (2017a) in the Peel Harvey region in Western Australia, Australia: site coordinates were 32° 48 826’S, 115° 53346’E and the site was ~8 m above sea level. The field contained winter-active annual grasses and legumes and supported a low-intensity free-range beef cattle grazing enterprise. Soil collection targeted a sandy loam soil with a pH in $CaCl_2$ of 5.4. Soil was wet-sieved through a stack of four sieves with pore sizes ranging from 2 mm down to 20 µm. The material collected on each sieve was retained and added to pasteurised, dried, washed coarse river sand at a ratio of either 1:27 or 1:81 w/w. Free-draining pots were filled with 1 kg of each treatment (n=4) and placed in a temperature-controlled glasshouse. Four plants of *T. subterraneum* L. with appropriate rhizobia added were grown in each pot which were

maintained at 80% field capacity by watering to weight, and received phosphorus-free, but otherwise complete, nutrient solution once a week. After 8 weeks, plants were harvested and roots gently washed clean. The four root systems from each pot were allocated to one of two future activities: staining for assessment of AMF colonisation (stored in 70% ethanol) or DNA extraction (frozen at -20ºC). Roots were cleared and stained using the ink-vinegar method of Vierheilig et al. (1998) and assessed using a modified version of the magnified intercept method described by McGonigle et al. (1990) where the root at each grid-line root intercept was recorded as either free of all colonisation, colonised by G-AMF only, colonised by M-AMF only, or colonised by both M-AMF and G-AMF.

DNA extraction, 18S rRNA gene amplicon sequencing and metagenome sequencing

Twelve samples were selected for 18S rRNA amplicon and metagenome sequencing on the basis of predominance and abundance of M-AMF colonisation as well as quality and quantity of DNA obtained (Table S1). DNA was extracted from root samples using the DNeasy PowerSoilPro Kit (Qiagen) following the manufacturer's protocol. DNA concentrations were measured using a Qubit 3.0 fluorimeter using the Qubit dsDNA high sensitivity assay kit (Invitrogen) according to the manufacturer's protocol.

To determine whether the dilution technique had enriched M-AMF we preformed community 18S rRNA amplicon analysis. Glomeromycotina and Mucoromycotina 18S rRNA genes in root samples were amplified using AM-Sal-F and AMDGR primers which amplify a 220-base fragment (Seeliger et al., 2024). PCR reactions, Illumina MiSeq sequencing, and bioinformatic analysis were performed using the approaches outlined in Seeliger et al. (2024).

Long read nanopore amplicon sequencing of the nuclear ribosomal 18S rRNA, 5.8S, and 28S/LSU region of Mucoromycotina was performed on root samples to support construction of the FRE MAG and to determine its phylogenetic relationships. PCR reactions were conducted using AM-Sal-F in combination with RCA95m (Wurzbacher et al., 2018) using the recommended Oxford Nanopore protocol, amplifying a 4.5 kb region. Briefly, an initial PCR was performed with adapter-tagged oligos, and the PCR products were cleaned using Ampure SPRI beads. Barcodes were added using a second PCR with an initial denaturation at 95ºC for 3 minutes followed by 30 cycles of denaturation at 98ºC for 15 seconds, 60ºC annealing for 15 seconds, and 65ºC extension for 150 seconds, with a final extension at 65ºC for 6 minutes. Following a clean-up with SPRI beads, the samples were used for sequencing on a SpotON Nanopore flow cell following the manufacturer's instructions.

Fast5 files were base called and demultiplexed using the Guppy basecaller provided by Oxford Nanopore Technologies. The sample was then processed using amplicon_sorter v2022-03-28 (Vierstraete & Braeckman, 2022) which aims to group amplicons at species or genus level (~95%), output consensus sequences, and quantify the copy number of the representative consensus sequences in the sample. This resulted in 42 consensus sequences, 5 of which were placed into the Mucoromycotina.

To aid detection of M-AMF sequences in the metagenome, a reference 18S rRNA sequence was obtained from DNA extracted from *T. subterraneum* root samples which were enriched in M-AMF and contained minimal G-AMF. These samples were produced in a similar manner to that described above and are presented in Orchard et al. (2017a) as "Experiment 1". On average, 90% of the total AMF colonisation in these roots was contributed by M-AMF, presenting the first evidence linking FRE morphology to Mucoromycotina. The AM-Sal-F and RCA95m primers were used to amplify a 4.5 kb region, as described above, which was cloned using the TA cloning kit (ThermoFisher). Partial 18S rRNA analysis using AM-Sal-F and AMDGR primers revealed a clone, FRE4583, whose sequence showed a 100 % match both to OTU4 which was associated with FRE morphology in the earlier Orchard et al. (2017) study and the BEG249 *Planticonsortium tenue* FRE culture described by Walker et al (2018) (Albornoz et al., 2022). Furthermore, this and closely related sequences have been detected in multiple studies reporting FRE morphology in plant roots (Albornoz et al 2020, Seeliger et al., 2024). Primer walking was used to sequence overlapping regions of clone FRE4583 until the full sequence was covered, generating a 4.5 kb fragment.

Metagenome sequencing and assembly

The twelve root samples were used for Shotgun metagenomic sequencing using the HiSeq 150 paired end protocol to generate between 15 and 47 Gbp sequencing depth. Library construction and sequencing was conducted using Illumina protocols by Novogene UK Ltd.

Samples were first filtered for *T. subterraneum* DNA using bwa mem v0.7.18-r1243-dirty (Li, 2013) and samtools v1.10 (Danecek et al., 2021). To determine FRE depth and breadth of coverage the filtered metagenome reads were mapped, again using bwa mem and samtools, against the FRE4583 ribosomal operon and the resulting alignment files processed with custom Python scripts. To be sure that a high mean coverage was not an artefact of conserved regions, breadth of coverage was visually inspected. Sample P72 was predicted to have the

highest Mucoromycotina abundance, possessing the majority of the operon with a coverage depth of over 100 (Fig. S1); the missing regions are likely due to repeats as we filtered ambiguous mappings. We therefore focussed on this sample in our efforts to reconstruct an M-AMF genome, assembling it using the SPAdes assembler v3.14.1 (Bankevich et al., 2012). This produced a catalogue of contigs with an N50 of 446 and total length of 1.3 Gbp. We then computed coverage depth profiles for these contigs across all samples by mapping reads with bwa mem, samtools, and bedtools v2.30.0 (Quinlan & Hall., 2010). This improves the discriminatory power of genome binning through multi-sample coverages whilst keeping the best quality single sample assemblies. The contigs were then binned using these coverage profiles and composition with the binning software CONCOCT v1.1.0 (Alneberg et al., 2014) and a minimum contig length of 1000bp.

The putative M-AMF genome was identified based on a consensus of multiple lines of evidence. As a first step, our reference M-AMF ribosomal sequence FRE4583 was mapped to the assembly. A total of 12 unitigs were found with high similarity (>98%) and spanning 75% of the operon without overlap, of which only four had a context in the assembly graph. Using custom scripts, co-localisation of contigs binned by CONCOCT within the direct vicinity of the aforementioned 4 untigs were visualised directly on the SPAdes assembly graph (Fig. S2) using Bandage v0.8.1 (Wick et al., 2015). This figure encompasses all paths of 10 Kbp starting from these 4 unitigs (red) but correspond to only 0.05% of the whole assembly, showing a clear proximity of multiple numbered bins. Ignoring any miss-assemblies, all genomes have a distinct path in the assembly graph and in particular the M-AMF genome should include a path which passes through those unitigs labelled as ribosomal sequences allowing us to identify the M-AMF, even though we could not assemble a complete FRE4583 operon in a single contig, likely due to strain diversity.

A total of 12 bins were found in close proximity to M-AMF unitigs. However, on assessing quality, only bin 17 was found to have any marker genes, giving it a completion of 83.7% using the BUSCO (Manni et al., 2021) general fungi_odb10 scheme with a size of 37.37 MBp (Table S2). In particular, while contigs from bin 70 were directly co-located with FRE ribosomal sequences, this bin did not possess any marker genes and was distinctly different in terms of coverage from bin 17. It may be that bin 70's location in the graph is due to a miss-assembly, or it could be that this is due to strain diversity and that bin 70 is strain-specific part of the pan-genome of the FRE which would result in it having a different coverage profile to the core genome represented by bin 17. To further confirm that bin 17 is related to

M-AMF, we used phyloFlash v3.4.2 (Gruber-Vodicka et al., 2020) to quantify ribosomal operon abundance from the 12 Illumina short read samples. It is indeed possible to use phyloFlash to derive abundance, not only of the SSU rRNAs of the SILVA database (Quast et al., 2013) but also of the 42 nanopore amplicon 18S rRNA consensus sequences. Filtering any taxa with less than 10 reads mapping across all samples yielded a total of 251 entries including the 42 consensus sequences (Fig. S3). These were normalised by the total sequencing depth of each sample. To compare to these, the coverage depth of bin 17 was calculated for each sample by taking the sum of all nucleotides mapping to all contigs of bin 17 and dividing by the total length of the contigs, followed by normalisation as above. Using Pearson's correlation, the coverage of bin 17 was compared to the coverage of all 251 taxa detected with phyloFlash. The strongest correlation was with one of the FRE consensus sequences (consensus_all_seqs_0_16). This was found to be correlated with $r = 0.97$ and an adjusted p value of 4.5e-11 (Fig. S4). The regression coefficient of 63 between coverage profiles (consensus_all_seqs_0_16 and bin 17) would imply that there are that many ribosomal operons in the genome, which is consistent with other fungi.

Reference genome access and ecological lifestyle annotation

To compare the MAG to known fungi, a database of reference fungal genomes was constructed from JGI MycoCosm (Table S3). The fungal species, representing the three phyla—Ascomycota, Basidiomycota, and Mucoromycota —were chosen based on two criteria. First, fungal genomes which had been included in previous comparative genomics analyses of mycorrhizal fungi (Martino et al., 2018; Miyauchi et al., 2020) were included since the ecology of these fungi had already been curated. Secondly, the database was supplemented with Mucoromycota genomes available in MycoCosm (https://mycocosm.jgi.doe.gov/mucoromycota/mucoromycota.info.html) in May 2023. The associated predicted fungal proteomes were accessed and downloaded in May 2023. We acknowledge that this was not an exhaustive list of fungal genomes accessible on JGI MycoCosm in that there were genomes representing further species within Ascomycota and Basidiomycota that were not included in the analyses. Additionally, with our primary focus being the provision of comparable context for the MAG, we aimed to obtain a broadly representative database and not an all-encompassing list.

Fungal genomes were categorised according to their ecological lifestyle (Table S3). To achieve this, fungal species were coded as follows. First, ecological classifications were accessed from functional groups recorded on JGI MycoCosm (e.g., https://mycocosm.jgi.doe.gov/Ectomycorrhizal_fungi/ Ectomycorrhizal_fungi.info.html). Secondly, for genomes which were included in previous comparative genomics analyses, the classifications reported in those studies were used (Chang et al., 2019, 2022; Martino et al., 2018; Miyauchi et al., 2020). Any remaining genomes without classifications were then manually curated, as informed by published evidence. Similarly to previous studies, we allowed a fungal species to occupy multiple ecological lifestyles when there was evidence of this. We assigned 146 genomes as saprotrophic, 42 as ECM, 29 as pathogenic, 23 as mixed lifestyle, 12 as G-AMF, 9 as endophytic, 5 as parasitic, 4 as ERM, 3 as OCM, and 1 as lichenic. Within this total we included the following five Mucoromycotina genomes. *Endogone* sp. 'Endsp1' is a putative saprotroph found on fallen oak logs in Florida, USA (Chang et al., 2019). *Jimgerdemannia lactiflua*, 'Jimlac1' is a putative ectomycorrhizal fungus isolated from under *Pseudotsuga menziesii* in Oregon, USA (Chang et al., 2019). Two genomes of the putative ectomycorrhizal fungus *Jimgerdemannia flammicorona*: isolate 'Jimfl_GMNB39_1' from under *Picea abies* and *Picea pungens* in Michigan, USA (Chang et al., 2019), and isolate 'Jimfl_AD_1' from under *Pinus strobus* in Biella, Italy (Chang et al., 2019). *Bifiguratus adelaidae* 'Bifad1', a soil-dwelling putative saprotroph isolated from a *Pinus taeda* plantation in North Carolina, USA (Torres-Cruz et al., 2017).

Phylogenetic assessment

Phylogenetic assessment of FRE4583 and those consensus sequences from root samples which were assigned to the order Endogonales (including all_seqs_0_16) was carried out through 18S rRNA gene alignment. These sequences were added to the Endogonomycetes 18S rRNA alignment from Tedersoo et al. (2024) using MAFFT v7.525 (Katoh and Standley, 2013). The resulting alignment was manually checked and refined in MEGA11 v11.0.13 (Tamura et al., 2021). The best fitting model for our alignment was selected using IQ-TREE v2.3.6 and the option "-MFP" (Kalyaanamoorthy et al., 2017; Minh et al., 2020). A phylogenetic tree was generated using the model "TIM2+F+R5" with 1000 approximate likelihood ratio tests and 1000 ultrafast bootstraps (Hoang et al., 2018; Minh et al., 2020). The tree was subsequently visualised in FigTree v1.4.4 (Rambaut, 2009).

In addition to the 18S rRNA alignment, fungal phylogeny was inferred from genome sequences using a concatenated protein marker alignment. A set of 434 protein markers identified by the JGI as pan-fungal markers for inferring high-level fungal phylogeny was used to compare the phylogenetic placement of the MAG and all the reference fungal genomes within our curated database. To identify these marker proteins, an HMM set was downloaded from https://github.com/1KFG/Phylogenomics_HMMs/tree/master/ HMM/JGI_1086. Phylogenomic markers were extracted from fungal proteomes using the above HMM, and a subsequent phylogenetic tree was built using PHYling v0.9.0 (available at: https://github.com/stajichlab/PHYling) under default settings. The tree was then visualised in R using ggtree v3.6.2 (Yu et al., 2017).

Annotation of MAG and reference genomes

Our comparative analyses focused on Carbohydrate-Active enZymes (CAZymes), lipases, proteases, transporters, and small-secreted proteins. To identify CAZymes, fungal proteomes were queried against an HMM profile database built from CAZy sequences downloaded from the dbCAN2 database (accessed from: https://bcb.unl.edu/dbCAN2/download/Databases/V11/dbCAN-HMMdb-V11.txt) (Zhang et al., 2018) using HMMer v 3.3.2 (Eddy, 2011). Protein hits were subsequently filtered with an e-value threshold of 1e-15 and an alignment threshold of 50% of the domain query. To identify proteases, fungal proteomes were queried against the MEROPS peptide database (accessed in July 2023 from: https://ftp.ebi.ac.uk/pub/databases/merops/current_release/merops_scan.lib) using BLASTp. Protein hits were subsequently filtered with an e-value threshold of 1e-10. To identify lipases, fungal proteomes were queried against the Lipase Engineering Database v4.1.0 using DIAMOND v2.1.8 (Buchfink et al., 2021) and the option “-sensitive”. Protein hits were subsequently filtered with an e-value threshold of 1e-5. To identify transporters, fungal proteomes were queried against the TCDB transporter database (accessed in November 2023) (Saier et al., 2021) queried using BLASTp. Protein hits were subsequently filtered with an e-value threshold of 1e-10. Secreted proteins were identified using a custom pipeline as reported previously (Pellegrin et al., 2015). Briefly, signal peptides were identified with SignalP v4.1 (Petersen et al., 2011), extracellular localisation was predicted with WoLFPSort v0.2 (Horton et al., 2007), transmembrane helices were identified with TMHMM v2.0 (Möller et al., 2001), secretory pathway association was inferred with TargetP v2.0 (Almagro

Armenteros et al., 2019), and the absence of a KDEL motif in the C-terminal region was confirmed with PS-SCAN revision 1.86 (De Castro et al., 2006). Small-secreted proteins were identified as secreted proteins < 300 amino acids with no CAZyme, lipase, protease, or transporter annotation. Functional annotation of putative small-secreted proteins was achieved with PfamScan v1.6 (Mistry et al., 2007), an e-value threshold of 1e-15, and an alignment threshold of 50% of the domain query. For each functional protein category being identified, a single best hit per locus was retained by selecting the hit with the smallest e-value and greatest alignment of the domain query.

Comparative genomics analyses

All comparative genomics analyses were conducted using R v4.2.2 (R Core Team, 2021), and all visualisations were generated with ggplot2 v3.4.0 (Wickham, 2016). Functional annotation of EC numbers was assigned using DeepECtransformer v1.0 (Kim et al., 2023) and the ECRECer web platform (Shi et al., 2023).

Results

Description of FRE in the roots

The appearance of the FRE in the roots of the twelve samples chosen for metagenomic sequencing was consistent with the description of the genus *Planticonsortium* by Walker et al. (2018) into which they placed *Glomus tenue* (previously generically referred to in the literature as fine endophyte or fine root endophyte; Orchard et al. 2017b) (see photographs in: Fig. 1 herein; Figure 2 and Figure S1 in Orchard et al., 2017a and Thippayarugs et al. (1999)). In particular, entry points were characterised by structures with “feather-like, fan-shaped, palmate or multilobed with finger-like projections” (Walker et al. 2018) which then led to fine, diverging hyphae in cortex cells and, often, plentiful finely-branched arbuscules. Small intercalary vesicles and terminal vesicles were also common. Droplets of lipids were often evident within hyphae and arbuscules. In some instance, colonisation in the cortex was too dense to clearly distinguish the structure of individual arbuscules.

In the samples used for amplicon and metagenome sequencing the percentage of total root length colonised AM ranging between 26.8 and 72.5% for AMF with FRE morphology and 0 to 16.3% for G-AMF, producing a proportion of AMF colonisation by FRE between 62.2 and

100%. 18S rRNA Miseq sequencing of Glomeromycotina and Mucoromycotina communities in root samples revealed that the proportion of Endogonales amplicons ranged between 25 and 82% (Table S1).

Phylogeny and Features of Fungal Genomes

In this study we constructed a putative FRE genome, referred to as the 'MAG'. This MAG was identified as a putative M-AMF through two lines of evidence. First, the contig bin was colocated on the assembly graph with unitigs that we could assign to the 18S rRNA gene of a known M-AMF reference (FRE4583). Secondly, its abundance correlated across the 12 samples in the study with an 18S rRNA sequence 'consensus_all_seqs_0_16', which we showed to be very closely related to FRE4583 (Fig. 2). The bin itself did not contain a complete 18S rRNA sequence. This is unsurprising as this gene is well known for failing to assemble, largely due to it being comprised of strongly conserved regions that repeat throughout the genome, failing to assemble into substantial contigs. The MAG measured 37.37 Mbp with a genome coverage varying between 1x and 568 depending on sample. The N50 was found to be 4928 with a GC content of 41.1%. Finally, its completion was assessed to be 83.7% with only 1.5% contamination (Table S2). We identified a total of 10872 proteins. Of these proteins, we were able to assign 3358 proteins with a functional annotation, comprising 218 CAZymes, 121 lipases, 280 proteases, 13 small secreted proteins, and 2726 transporters.

While we acknowledge that the revised phylogeny of the Mucoromycotina subphylum produced in Tedersoo et al. (2024) lacks type specimens and is grounded in part on dark taxa, as a poorly captured branch of the fungal tree of life we deem this an appropriate basis to apply the phylogeny of our MAG. 18S rRNA analysis placed consensus_all_seqs_0_16, and by proxy the MAG, within the order Densosporales of the Mucoromycotina, corresponding with the Densosporaceae sensu Desirò et al. (2017) (Fig. 2). This order is associated with FRE morphology (Orchard et al., 2017a; Chang et al., 2019). Further to this, strong support values allow us to confidently place the MAG in the newly proposed family *Planticonsortiaceae* (Tedersoo et al., 2024). Within this family, the MAG was placed with very high similarity to the known M-AMF reference sequence, FRE4583 (Fig. 2). Further to this, the MAG was closely related with three other Mucoromycotina 18S rRNA sequences obtained from the root samples (consensus_all_seqs 0105, 0122 and 0260) and to environmental sequences obtained from the thalli of early diverging plant sequences, e.g., MH174585 and MH174471. The wider *Planticonsortiaceae* clade included further sequences

from the thalli of non-vascular plants, sequences not annotated beyond the phylum level associated with soil from across Europe (EUK sequences), and one sequence associated with the rhizosphere of *Populus tremuloides* (EF23703), a known arbuscular mycorrhizal host (Lee et al., 2020). Phylogenetic analysis therefore placed the MAG apart from other members of the Mucoromycotina with putative ecology from the order Endogonales, including the putative ectomycorrhizal Mucoromycotina member *Jimgerdemannia* spp. (Desirò et al., 2017) and the saprotrophic *Endogone* sp. and *Vinositunica* sp. which have a putative saprotrophic or ectomycorrhizal lifestyle (Yamamoto et al., 2020).

Similarly, the protein marker alignment placed the MAG within the Mucoromycota (Fig. 3). The closest relatives are within the order Endogonales, including *Endogone* sp. and *Jimgerdamannia* spp, since no Densosporales genomes are available to date. The MAG forms a sister clade relative to *Endogone* and *Jimgerdamannia*, suggesting it diverged early from the other Mucoromycotina.

Genomic Profile of the MAG

To contextualise the gene content of the MAG, we compared the CAZyme, protease, lipase, and transporter profile to genomes within the reference dataset that represented the saprotrophy-symbiont continuum. We also compared the MAG with the five available genomes from the Endogonales, which the 18S rRNA and genome analysis confirmed as the closest phylogenetic relatives to the MAG. The ecological lifestyle had a significant effect on genome content across all four categories ($p < 0.01$) (Fig. 4). For the CAZymes, the ecological lifestyles fell into two groups—G-AMF and ECM, ERM and OCM —with SAP bridging the two (Fig. 4a). The MAG contained a low number of CAZymes (218), which was similar to the mean of the ECM (240), but slightly higher than that of the G-AMF (175). A similar number of CAZymes were found in the MAG compared to related Endogonales genomes (149 to 208). The ERM genomes contained by far the largest median number of CAZymes across the lifestyles (629). Only the ERM possessed a significantly ($p < 0.01$) larger number of lipases than the other ecological lifestyles (Fig. 4b). The MAG possessed 121 lipases, lower than the means of the G-AMF (189), ECM (238), and SAP (263), OCM (268). Similarly, the related Endogonales genomes all contained low numbers of lipases (72 to 132). The ERM genomes had significantly ($p < 0.01$) higher mean numbers of proteases per genome (457) than the other lifestyles (Fig. 4c). The MAG had similar numbers of proteases (280) compared to G-AMF (305), ECM (286), SAP (271), and to the related Endogonales genomes (229 to 298). The G-AMF and ERM lifestyles had significantly higher

($p < 0.05$) numbers of transporters per genome relative to the other genomes. The MAG (2726) had a substantially lower number of transporters compared to G-AMF (3900); however, it contained more than related Endogonales genomes (1932 to 2388) that sat in the lower end of the dataset (Fig. 4d). Across the dataset, the saprotrophs contained an especially high degree of intra-group variability in numbers of all four profiles compared to the other ecological lifestyles (Fig. 4). The number of CAZymes, lipases, proteases, and transporters in the MAG were also comparable to the endophyte, parasite pathogen, and mixed lifestyles (Fig. S5). The MAG contained 13 small secreted proteins, a middling amount for the dataset (Fig. S5).

CAZyme Profile

CAZyme proteins associated with the degradation of plant and microbial cell walls were identified to investigate the saprotrophic repertoire of the MAG, in the context of the mycorrhizal saprotrophy-symbiont continuum. The ERM (252) and OCM (215) genomes possessed a significantly higher ($p < 0.01$) mean number of PCWDEs than the G-AMF (32), ECM (59), and SAP (77) genomes (Fig. 5a). The MAG contained a similar number of PCWDE (37) as the G-AMF genomes and the genomes of related Endogonales (33 to 44), which was notably lower than the endophyte, parasite, pathogen, and mixed lifestyles (Fig. S6). ERM genomes contained a significantly ($p < 0.01$) higher mean number of MCWDE (109) than the saprotrophs and other mycorrhizal lifestyles (24 to 59) (Fig. 5b). The G-AMF genomes had a significantly ($p < 0.05$) lower number of MWCDE (24) compared to the mean ECM (45), OCM (59), and SAP (48) genomes. The MAG had 53 MCWDE, higher than the median number of all other lifestyles except the ERM (Fig. 5b, Fig. S6), and similarly higher than numbers in the parasite, pathogen and mixed lifestyles, but similar to numbers in endophytes (Fig. S6). A similar number of MCWDE was detected across the Endogonales genomes (36 to 53).

Patterns of PCWDE distribution across the mycorrhizal associations were similar (Fig. 6). ERM and OCM genomes had significantly ($p < 0.01$) higher mean numbers of cellulases, hemicellulases, and pectinases than the G-AMF and ECM genomes. Relative to the mean G-AMF, the MAG had notably higher numbers of cellulases (18 compared to 8), but similar numbers of hemicellulases (11 compared to 7) and pectinases (4 compared 2). The Endogonales genomes had similar numbers of cellulases (11 to 13), hemicellulases (10 to 16), and pectinases (4 to 12) as the MAG. The numbers of lignin degrading enzymes were significantly higher in the ERM (31, $p < 0.01$) relative to the other mycorrhizal lifestyles,

which all possessed similar numbers: ECM (13), G-AMF (15), OCM (9), and SAP (12). Notably the MAG had a very low number of lignin degrading enzymes (4) compared to all other lifestyles, this trend was consistent across the other Endogonales genomes (2 to 8). Numbers of cellulose, hemicellulose, and pectin degrading enzymes in the MAG were also typically lower than the mean in endophyte genomes (Fig. S7), and numbers of lignin degrading genes were similarly notably lower than the endophyte, parasite, pathogen and mixed lifestyles (Fig. S7).

Cellulases in the MAG genome comprised 8 families, with 6 copies of AA9 being the most abundant (Table S4). The other Endogonales genomes contained an average of 6 cellulase families, with GH9 being the most abundant in all four genomes, of which the MAG contained 3. However, not a single copy of AA9 was identified within the other Endogonales genomes (Table S4). The G-AMF genomes only contained an average of 3 families, with the Glomerales containing a mean of just 6 cellulases. However, the Diversisporales contained a much higher number of cellulases (17 and 12), including 7 and 6 of AA9 and 6 and 3 copies of AA3, respectively (Table S4). The MAG contained a full suite of cellulose degradation enzymes: Endoglucanase, β-glucosidase, and exoglucanase (Table S5). However, with the absence of β-glucosidases in all G-AMF genomes and only two containing a single copy of exoglucanase, none of the G-AMF genomes possessed the full cellulose degradation pathway (Table S5). Hemicellulases in the MAG comprised the majority of the remaining PCWDEs, with 7 families and 5 copies of GH31 being the most abundant (Table S4). Similarly, the other Endogonales genomes contained an average 8 families, with GH31 being the most abundant. The G-AMF genomes contained an average 3 families, with GH31 and GH5_7 being the most abundant (Table S4). No copies of GH29 or GH95 were found within the G-AMF genomes. Similarly, no copies of GH95 were found within the MAG. However, a single copy of GH29 was present (Table S4).

Pectinases in the MAG were limited, with only 4 copies across 3 families: 2 GH35s, 1 GH2, and 1 PL1_7 (Table S4). The other Endogonales genomes contained an average of 4 families, with the most abundant being GH28 and GH35 (Table S4). Within the G-AMF genomes, no evidence for pectinases was found within ‘Gigmar1’. Apart from that, all other genomes contained only 2 or 3 copies of GH35 (Table S4).

The MAG contained 3 families of lignin degrading enzyme: 2 AA1, 1 AA1_2, and 1 AA2 (Table S4). This trend was conserved across the Endogonales genomes, in which lignin

degrading enzymes comprised of 3 families, with AA1 being slightly more abundant (Table S4). The G-AMF genomes, while only comprising an average 3 families, contained a much larger number of lignin degrading enzymes. The Diversisporales contained 37 and 25 lignin degrading enzymes, including 35 and 23 copies of AA1 respectively. The Glomerales contained an average of 12 lignin degrading enzymes per genome, with an average of 9 counts being attributed to AA1 (Table S4).

The G-AMF genomes had a smaller mean chitinase repertoire (16) than ERM (35, $p < 0.01$), OCM (25, $p < 0.05$), and SAP (26, $p < 0.01$) (Fig. 7a). However, the MAG had one of the highest numbers of chitinases across the genome database (38), roughly double the mean number found in both the G-AMF and ECM (21), and notably higher than the mean found in endophytes, parasite, pathogen, and mixed lifestyles (Fig. S8). However, there was considerable variation in the numbers of chitinases across the G-AMF genomes, with the two Diversisporales genomes containing 38 and 29 counts respectively, more comparable to the MAG. The Endogonales genomes similarly contained high mean numbers of chitinases (29 to 42) compared to other genomes in the dataset. Over half of the MAG's chitinase repertoire was attributed to just two families, CE4 and GH18, with 16 and 13 copies respectively, a trend also seen across the other Endogonales genomes (Table S4). The G-AMF genomes largely comprised of CE4 chitinases, however, the Diversisporales genomes also contained a large number of GH18 (13 and 10), very few of which (0 to 2) were found in Glomerales (Table S4). The MAG contained a fully comprehensive set of chitin degrading enzymes (Table S5). Similarly, all but one of the G-AMF genomes contained a full chitin degradation suite (Table S5).

G-AMF genomes contained significantly ($p < 0.01$) lower mean numbers of glycan degrading genes (1) compared to the mean of the saprotroph (14) and other mycorrhizal lifestyles (15 to 42), and in fact were only detected in the two Diversisporales genomes (Fig. 7b). In contrast, the MAG contained 3 glycanases, and this was consistent with a low number of glycanases in the Endogonales genomes (2 to 8). The MAG only contained 2 copies of GH17 and 1 copy of GH5_9 (Table S4). The only two other genomes to contain single copies of these were 'Jimfl_AD_1' and 'Jimfl_GMNB39_1'. All the other Endogonales genomes contained 1 or 2 copies of both GH72 and GH81 (Table S4). The Diversisporales genomes only contained low counts of GH5_9 and GH81 (Table S4).

ERM genomes contained a higher mean number of mannanases (24) than the saprotrophic and other mycorrhizal lifestyles (3 to 6) (Fig. 7c). However, the MAG contained a

substantially higher mean number of mannanases (9) than the G-AMF (3) and ECM (5), and also the Endogonales genomes (2 to 4). Similarly, there was a range of mannanases across the G-AMF genomes with the two Diversisporales genomes containing 11 and 10 counts respectively, more comparable to the MAG (Table S4). The MAG again contained a comparatively large set of genes for mannan degradation, with 5 copies of GH92, 3 copies of GH125, and 1 copy of GH76. However, this represents the one substrate-specific group that was not as conserved across the phylogenetically closest relatives. None of the Endogonales genomes contained copies of GH76, while all contained 1 or 2 copies of CE17 (Table S4). Additionally, while three of the four contained GH92, it was only in single-copy instances. The G-AMF genomes showed a range of mannanases within their genomes, and particularly the Diversisporales genomes alone contained many copies of GH92. All but one Glomerales genome only contained 1 or 2 copies of GH125, with no mannaanase identified in the 'RhiirC2' genome (Table S4).

Low numbers of peptidoglycanases were found in the genomes of all lifestyles, with significantly larger mean numbers in ERM (8, $p = <0.01$) compared to the ECM (3) and saprotroph (2) genomes (Fig. 7d). The G-AMF genomes had a comparable mean number of peptodoglycanases (4) to the MAG (3), while the corresponding numbers in the Endogonales genomes were also low (0 to 3). The MAG only contained 2 copies of GH24 and a single copy of GH89 (Table S4). Similarly, the other Endogonales genomes were sparse in peptidoglycanases. Specifically, the 'Jimfl_GMNB39_1' genome contained no peptidoglycanases, while 'Jimfl_AD_1' and 'Jimlac1' only possessed a single copy of GH89 and CMB50, respectively. 'Endsp1' also contained 2 copies of CBM50 and a single copy of GH24. The G-AMF genomes also contained a small number of peptidoglycanases, mostly consisting of GH24 (Table S4).

The MAG contained no genome-specific cell wall degrading enzymes families. However, a poorly described GH151 family, "α-L-fucosidase enzyme encoding protein", was only identified within 3 of the closest phylogenetic relatives (Jimfl_AD_1, Jimfl_GMNB39_1, and Endsp1) and a far-removed saprotrophic basidiomycete, Dacsp1 (Table S4).

Transporters

Since the ability to transport nutrients and assimilate with the host plant is core to the lifestyle of a fungal symbiont, we compared substrate-specific transporters between the ecological lifestyles. Only the ERM genomes contained a statistically higher ($p = 0.044$) number of

phosphate transporters than the other genomes (Fig. 8a). The MAG contained a relatively low number of phosphate transporters (14), although this was not too dissimilar from the mean of the G-AMF (18) and the same as the mean ECM genome (14). Similarly, the Endogonales genomes possessed low numbers of phosphate transporters (13 to 15) (Fig. 8a). The G-AMF genomes had a significantly higher ($p < 0.01$) number of calcium transporters (55) compared to the other mycorrhizal and saprotrophic lifestyles (Fig. 8b, which ranged between 26 and 39), and also the endophyte, parasite, pathogen, and mixed lifestyles (Fig. S9). The MAG showed a similar number of calcium transporters (50) to the G-AMF, while the number of calcium transporters in the Endogonales genomes varied considerably (25 to 47) (Fig. 8b). There was no significant difference ($p = 0.48$) in the number of copper transporters across the mycorrhizal and saprotrophic genomes, with the mean varying between 13 and 17 (Fig. 8c). However, the MAG contained only 6 copper transporters, one of the lowest of all genomes (Fig. 8c, Fig. S9). Of the Endogonales genomes, 'Jimlac1' had the second smallest number of copper transporters (7) while the rest ranged from 8 to 13 (Fig. 8c). The G-AMF had a significantly higher ($p < 0.01$) number of nitrate transporters (7) compared to the other mycorrhizal and saprotrophic lifestyles (Fig. 8d). The MAG contained a low number (2) of nitrate transporters relative to the mean G-AMF, although this was the same as the mean ECM (2) and similar to the ERM (3), OCM (1), and SAP (1). There was considerable variation in the mean number of nitrate transporters within the Endogonales genomes (0-5) (Fig. 8d). The ERM genomes had a significantly higher ($p < 0.01$) mean number of ammonium transporters (11) than all but the G-AMF genomes (9) (Fig. 8e). The MAG contained 5 ammonium transporters, slightly higher than the median ECM (4) and OCM (4). The MAG contained an especially low number of glycine transporters (1), the same as the average ECM (1) and OCM (1) genome (Fig. 8f). The ERM contained the highest mean number of glycine transporters (5), whereas the G-AMF (3) and SAP (4) were not significantly different to any of the other ecological lifestyles (Fig. 8f).

Hallmark Missing Glomeromycotan Core Genes

We analysed both the MAG and G-AMF genomes for enzymes linked to pathways that are missing from typical G-AMFs, often referred to as 'Missing Glomeromycotan Core Genes' (MGCG). As fatty acid auxotrophs, G-AMF have been shown to lack the presence of cytosolic fatty acid synthases required for fatty acid biosynthesis. We found no evidence of proteins directly associated with the fatty acid synthase required to facilitate fatty acid biosynthesis within either the G-AMF genomes or the MAG. We did identify 3-oxoacyl-ACP

reductase in all genomes, including 10 within the MAG. (Table S5). Additionally, neither the MAG nor the G-AMF genomes possessed the ability to biosynthesis thiamine, a hallmark of G-AMF genomes. Specifically, we found no evidence of the presence of thiamine phosphate synthase or hydroxymethylpyrimidine kinase (Table S5).

The ability to synthesis all derivatives of the vitamin B6 pathway was present within the MAG. This included a copy of pyridoxine kinase (2.7.1.35), the most prolific enzyme within the vitamin B6 metabolism pathway. Only one enzyme, pyridoxine 4-dehydrogenase, was missing from the pathway, while an indirect three-step metabolism for the conversion of pyridoxal to pyridoxine was present. Conversely, no G-AMF genome possessed a full vitamin B6 metabolism pathway, with no evidence of pyridoxine kinase being found across the group (Table S5).

Discussion

In the current work we assembled the genome of a putative FRE-forming AMF from a root metagenome. Methodologically this is a relatively unique achievement: fungal MAGs have been obtained previously from host associated environments and niche environments, but not from complex environments, such as the rhizosphere (Tagirdzhanova et al., 2021; Shen et al., 2023; Singh et al., 2023), or from similar fungal symbionts. To achieve this, we had to augment standard binning methods with assembly graph visualisations and coverage correlations to known M-AMF 18S rRNA genes. We believe that this method has many advantages over isolation and culturing, in particular it is less time consuming and in principle may be more reflective of the actual community present particularly if multiple species are present.

Phylogenetic analysis of the correlative 18S rRNA marker, consensus_all_seqs_0_16, showed that the MAG sits within the order Densosporales of the Mucoromycotina. The MAG represents the first published genome of both the order Densosporales and the family Planticonsortiaceae. The most closely related taxa with sequenced genomes are putative ectomycorrhizal and saprotrophic fungi from the order Endogonales, although a reasonable degree of dissimilarity is evident. The MAG was closely related to environmental sequences from the rhizoids of liverworts, which form arbuscular-like symbioses involving Glomeromycota and Mucoromycotina (Rimmington, 2018). To date, understanding of the phylogeny of fungi which form mycorrhizas with FRE morphology in vascular plants has

been restricted to short 18S rRNA fragments. Similarly, these studies have confirmed close phylogenetic relatedness with sequences from liverwort thalli (Orchard et al., 2017; Albornoz et al., 2021, 2022; Seeliger et al., 2024), suggesting these fungi form associations with both vascular and non-vascular plants, with a role in N and P nutrition of the plant host (Orchard et al, 2017a; Hoystead, 2023). Mucoromycotina sequences associated with plant roots may span both the Densosporales (Orchard et al., 2017b; Desirò et al., 2017; Chang et al., 2018) and Endogonales (Seeliger et al., 2024), and furthermore diverse assemblages of fungi from these orders may be present in roots (Seeliger et al., 2024), although fungi associated with the FRE morphology appear to be phylogenetically distinct from putative ectomycorrhizal and saprotrophic Endogonales (Seeliger et al., 2024).

Comparative genome analysis showed that the MAG's genome had many features in common with G-AMF. Some of these genomic features, including the low abundance of PCWDE and the absence of thiamine biosynthesis genes, were also seen in related Endogonales genomes and therefore aren't likely to be specific, hallmark features of an adaptation to a symbiotic lifestyle. However other signatures the MAG shares with G-AMF, including a high abundance of calcium transporters and the absence of fatty acid synthases, may point to physiological convergence in the way in which the symbioses operate. There were some notable differences between the MAG and G-AMF, with the MAG possessing a high abundance of chitinases, a complete vitamin B6 biosynthesis pathway, and low abundances of nitrate, ammonium and copper transporters. These features may point to differences between G-AMF and M-AMF in the way they interact with the host plant and the wider environment.

It has been suggested that the transition from saprotrophic to mycorrhizal lifestyles involved loss of PCWDE, enabling fungi to exist within roots without digesting them (Miyauchi et al., 2020). The G-AMF symbiosis is estimated to have evolved 450 mya, and Glomeromycotan genomes possess substantially lower numbers of these genes than the fungi forming the more recently evolved ectomycorrhizal, ericoid mycorrhizal, and orchid mycorrhizal symbioses. Furthermore, G-AMF show signatures of dependence on host metabolism that are absent from more recently evolved symbioses, including fatty acid auxotrophy and an inability to synthesise thiamine and metabolise vitamin B6 (Miyauchi et al., 2020). These represent the 'Missing Glomeromycota Core Genes' (MGCG, Tang et al., 2016; Kobayashi et al., 2018; Rosling et al., 2024).

Although genomic evidence indicates that G-AMF and M-AMF have independent origins (Rosling et al., 2024), these symbioses co-occurred in the earliest land plants (Strullu-Derrien et al., 2014), and they continue to co-occur in roots of extant plants (Orchard et al., 2017a). Additionally, while G-AMF and M-AMF exhibit some niche differentiation, evidence of overlapping ecological presence and similar responses to overarching edaphic and environmental variables have been noted (Albornoz et al., 2022; Seeliger et al., 2024). Furthermore, ultrastructural evidence points to similarities in the way in which G-AMF and M-AMF function at a cellular level (Albornoz et al., 2020). Therefore, similar evolutionary pressures may have acted on these symbioses, which could have resulted in convergence of genomic traits. Indeed, many of the symbiotic genomic features shown by G-AMF were also displayed by the MAG. This included a reduced repertoire of PCWDE and the absence of several MGCG, including those related to thiamine and fatty acid biosynthesis.

Our analysis confirms the findings of Rosling et al. (2024) that Endogonales have a low genomic PCWDE count and an incomplete thiamine biosynthesis pathway, suggesting that these may be features common to both the Densosporales and Endogonales, rather than an adaptation to biotrophy. However, the Endogonales genomes possess fatty acid biosynthesis genes (Rosling et al., 2024), so this signature of biotrophy does likely represent the same adaptation to biotrophy in G-AMF and M-AMF, which suggests that host assimilate is provided as fatty acids in both symbioses.

The MAG had a number of features which distinguished it from G-AMF genomes. In particular, while there was a shared low abundance of CAZymes, the MAG possessed a greater repertoire of enzymes for degradation of organic substrates than typically seen in G-AMF genomes. This included the full complement of enzymes required for degradation of cellulose, which was absent in all G-AMF genomes. In notable contrast to G-AMF, the MAG had a high count of both chitin and mannan fungal cell wall degrading enzymes. The high chitinase count doesn’t appear to be specific to the M-AMF, with the putative ectomycorrhizal and saprotrophic *Endogonales* genomes showing a similar pattern, attributed to elevated numbers of CE4 and GH18, as seen previously in Rosling et al. (2024). However, the full complement of chitinases was present in the G-AMF genomes as well as in the MAG, so this feature may not have any functional significance. Relative to other mycorrhizal fungi (except ericoid mycorrhizal fungi), the MAG had a notably high count of genes for mannan degradation. These were absent or present in low numbers in most G-AMF genomes and, significantly, were also found in low abundance in the *Endogonales* genomes, therefore high

abundance of mannan degradation genes may represent a distinguishing feature of FRE genomes. However, even within the G-AMF there appears to be some variation, with the *Diversisporales* genomes containing a higher number of mannan and chitin degrading enzymes than the *Glomerales* genomes, indicating a substantial range of genomic repertoires.

It is important to understand whether these contrasting enzymatic profiles contribute to niche partitioning between G-AMF and M-AMF in nutrient mobilisation from contrasting mineral and organic substrates. For example, high abundance of chitin and mannan degrading genes could indicate a role for M-AMF in the degradation of fungal necromass, while a complete cellulose degradation pathway and high abundance of cellulose and hemicellulose degrading enzymes could suggest involvement in saprotrophic breakdown of plant-derived materials, similar to some ECM fungi (Janusz et al., 2017; Martin & van der Heijden., 2024). Alternatively, it could reflect different strategies for enzymatic degradation of plant cell walls as they colonise and grow through host plant tissues and penetrate root cells.

Currently there is no indication that soil organic matter has any influence on the distribution of G-AMF or M-AMF. In contrast to G-AMF, evidence indicates that M-AMF are more abundant in agricultural than natural habitats, indicating a preference for low organic matter soils (Albornoz et al., 2022). However, these functional differences could support niche partitioning within these habitats.

A further distinguishing feature between the MAG and the G-AMF genomes is the presence of a full B6 biosynthesis pathway in the MAG, including pyroxidine kinase, which was missing in all the G-AMF genomes, as demonstrated in earlier studies (Tang et al., 2016; Kobayashi et al., 2018). B6 is a cofactor required for amino acid biosynthesis, and it also plays a role as an antioxidant. Reactive oxygen species (ROS) scavenging systems such as B6 may be required by AMF to overcome host defences, allowing intracellular colonisation and the development of arbuscules (Belmondo et al., 2016; Lanfranco et al., 2018). Components of the B6 biosynthesis pathway that G-AMF do possess are expressed throughout the fungal life cycle, but they are at the highest expression levels within the root (Benabdellah et al., 2009). Similarly, B6 plays a role in supporting the infection of root tissues by pathogens (Wang et al., 2023). Differences in capacity for independent production of B6 between the MAG and G-AMF could point to differences in the way the fungi scavenge ROS, and potentially also differences in the way root colonisation and arbuscule development are regulated by the plant. There could also be implications for the specific mechanisms underlying M-AMF and G-AMF responses to external stressors which generate ROS such as

temperature, osmotic stress, and nutrient limitation, and the independence of these responses to the plant's own response (Sahu et al., 2022).

Key physiological traits associated with G-AMF symbioses are the uptake of P from the soil, its translocation through hyphae to the root, and its transfer to the plant in exchange for carbon. Ultrastructural (Albornoz et al., 2020) and experimental evidence (Orchard et al., 2017b) suggest a similar role for M-AMF. A number of P transporters have been identified in G-AMF involved in P assimilation from soil, storage of P, and exchange of P with the host (Javot et al., 2006; Harrison et al., 2010; Plassard et al., 2019). G-AMF genomes generally showed higher mean numbers of P transporters than ECM, while numbers in the MAG were low relative to other mycorrhizal genomes studied. While the significance of transporters to the functioning of symbionts will depend on a range of factors including their efficiency, our data doesn't provide genomic support for particular specialisation in P nutrition by M-AMF.

Evidence also points to a potential role for G-AMF in N nutrition (Gosling et al., 2013). Indeed, G-AMF genomes contained higher numbers of nitrate transporters than the other mycorrhizal symbionts, while also sitting towards the higher end of both ammonium and glycine transporters within the genomes we analysed. However, further evidence of inter-group differentiation can be seen across the Diversisporales and Glomerales genomes, with the former containing especially high numbers of ammonium and glycine transporters. The MAG contained a lower number of all three categories of N transporters than all G-AMF genomes. While the MAG contained a typical number of ammonium transporters compared to the other mycorrhizal lifestyles, it contained a low number of nitrate and glycine transporters. Hoystead et al. (2023) suggested that M-AMF and G-AMF have complementary roles in host nutrition, with M-AMF predominantly involved in supply of N to the host and G-AMF in supplying P. Furthermore, Howard et al. (2024) showed a putative M-AMF displaying both a preference for, and increased transfer of, glycine and ammonium derived nitrogen sources. While there is evidence for the ability to transport varying forms of N, our MAG does not provide exceptional evidence for this relative specialism.

The very low abundance of Cu transporters in the MAG - the lowest across the entire dataset - is particularly striking. The three ectomycorrhizal Endogonales genomes also contain low numbers of Cu transporters, however the saprotrophic Endogonales sit near the mean. G-AMF may promote Cu uptake by the host plant (Taylor et al., 2015) and arbuscules have high demands for Cu (Gomez-Gallego et al., 2019). Furthermore, Cu transporters in G-AMF show differential expression profiles across intra- and extra- radical mycelium (Gomez-Gallego et

al., 2019). The extent to which M-AMF are involved in the supply of micronutrients to the host remains to be determined, but the evidence presented here could indicate that in contrast to G-AMF, this may not be an important function for M-AMF.

The high number of calcium transporters in both the MAG and G-AMF is a clear point of similarity between them, and of differentiation to all other groups. AMF have been implicated in transport of Ca to host plants (e.g. Liu et al., 2002), and our data could therefore indicate a role for both G-AMF and M-AMF in this function. However, Ca may also play a key role in the arbuscule lifecycle of both FRE and G-AMF. A clear link between a dramatic increase in calcium accumulation and arbuscule collapse has been demonstrated within G-AMF by both Ryan et al. (2003) and Sujkowska-Rybkowska and Znojek (2018). A similar trend within FRE was documented by Gianinazzi-Pearson et al. (1981) and Albornoz et al. (2020). While it is unknown whether the Ca accumulated originates from the host plant or the fungi, the high number of Ca transporters within both G-AMF and the MAG may indicate that Ca accumulation is driven by the fungal symbionts, perhaps depositing Ca to cease the function of the arbuscule once it reaches maturity.

Genome analyses, including those reported here, have identified differences across G-AMF which suggest contrasting interactions with the host and the wider environment. For both G-AMF and M-AMF, comprehensive analysis of genomic functional gene repertoires across the broad range of taxa found within roots is key to understanding the way that AMF communities support plant health, and the potential for engineering communities to promote beneficial traits. With the development of third generation long read sequencing technologies, genome assembly from metagenomes represents a promising route for understanding functions and traits associated with dark taxa in complex microbial communities, especially when combined with transcriptome sequencing (Benoit et al., 2024) to understand the factors which regulate gene expression within plant tissues and the soil.

Acknowledgements

We thank the Natural Environment Research Council (Grant NE/S010270/1), the Biotechnology and Biological Sciences Research Council (BBSRC) Midlands Integrative Biosciences Training Partnership (Grant BB/T00746X/1) and the Australian Research Council (Discovery Project DP180103157) for funding.

Competing interests

None declared.

Author contributions

GB, MHR, and CQ conceived the work and with RM obtained funding. MHR and PAD conducted the M-AMF enrichment work and the assessment of M-AMF colonisation of plant roots. SH, SR, and GB conducted sequencing and analysis of 18S rRNA genes. SR and CQ assembled the MAG. RHN, GM, and JC conducted the 18S rRNA gene phylogenetic analysis. JC, GM, SR, and GB performed the comparative genomic analyses. JC and GB wrote the manuscript. All authors edited the manuscript.

Data Availability

Raw 18S rRNA Miseq sequences are available at NCBI (BioProject ID PRJNA1179892), and Nanopore sequences at ENA (Experiment Accession ERX13330708). The FRE4583 sequence is available at NCBI (SUB14894546). The 18S rRNA phylogeny sequence alignment FASTA file and Newick tree file are available on PlutoF Biodiversity Platform (https://dx.doi.org/10.15156/BIO/3301225). The sequence of the MAG has been deposited on the Zenodo repository (https://doi.org/10.5281/zenodo.14144746).

References

Albornoz FE, Hayes PE, Orchard S, Clode PL, Nazeri NK, Standish RJ, Bending GD, Hilton S, Ryan MH. 2020. First cryo-scanning electron microscopy images and X-ray microanalyses of mucoromycotinian fine root endophytes in vascular plants. *Frontiers in Microbiology* 11: 2018.

Albornoz FE, Orchard S, Standish RJ, Dickie IA, Bending GD, Hilton S, Lardner T, Foster KJ, Gleeson DB, Bougoure J et al. 2021. Evidence for niche differentiation in the environmental responses of co-occurring mucoromycotinian fine root endophytes and glomeromycotinian arbuscular mycorrhizal fungi. *Microbial Ecology* 81(4): 864-873.

Albornoz FE, Ryan MH, Bending GD, Hilton S, Dickie IA, Gleeson DB, Standish RJ. 2022. Agricultural land-use favours Mucoromycotinian, but not Glomeromycotinian, arbuscular mycorrhizal fungi across ten biomes. *New Phytologist* 233(3): 1369-1382.

Alneberg J, Bjarnason BS, de Bruijn I, Schirmer M, Quick J, ljaz UZ, Loman NJ, Andersson AF, Quince C. 2014. Binning metagenomic contigs by coverage and composition. *Nature Methods* 11: 1144–1146.

Almagro Armenteros JJ, Salvatore M, Emanuelsson O, Winther O, von Heijne G, Elofsson A, Nielsen H. 2019. Detecting sequence signals in targeting peptides using deep learning. *Life Science Alliance* 2(5): e201900429.

Bankevich A, Nurk S, Antipov D, Gurevich AA, Dvorkin M, Kulikov AS, Lesin VM, Nikolenko SI, Pham S, Prjibelski AD et al 2012. SPAdes: a new genome assembly algorithm and its applications to single-cell sequencing. *Journal of Computational Biology* 19(5): 455-477.

Begum N, Qin C, Ahanger MA, Raza S, Khan MI, Ashraf M, Ahmed N, Zhang L. 2019. Role of arbuscular mycorrhizal fungi in plant growth regulation: implications in abiotic stress tolerance. *Frontiers in Plant Science* 10: 1068.

Belmondo S, Calcagno C, Genre A, Puppo A, Pauly N, Lanfranco L. 2016. NADPH oxidases in the arbuscular mycorrhizal symbiosis. *Plant Signaling & Behavior* 11(4): e1165379.

Benabdellah L, Azcón-Aguilar C, Valderas A, Speziga D, Fitzpatrick TB, Ferrol N. 2009. GintPDX1 encodes a protein involved in vitamin B6 biosynthesis that is up-regulated by oxidative stress in the arbuscular mycorrhizal fungus *Glomus intraradices*. *New Phytologist* 184(3): 682-693.

Benoit G, Raguideau S, James R, Phillippy AM, Chikhi R, Quince C. 2024. High-quality metagenome assembly from long accurate reads with metaMDBG. *Nature Biotechnology* 42: 1378–1383.

Brundrett MC, Tedersoo L. 2018. Evolutionary history of mycorrhizal symbioses and global host plant diversity. *New Phytologist* 220(4):1108-1115.

Brundrett MC. 2006. Understanding the roles of multifunctional mycorrhizal and endophytic fungi. In: BJE Schulz, CJC Boyle, TN Sieber, eds. *Microbial Root Endophytes*. Berlin, Germany: Springer-Verlag, 281–293.

Buchfink B, Reuter K, Drost HG. 2021. Sensitive protein alignments at tree-of-life scale using DIAMOND. *Nature Methods* 18: 366-368.

Chang Y, Desirò A, Na H, Sandor L, Lipzen A, Clum A, Barry K, Grigoriev IV, Martin FM, Stajich JE et al. 2019. Phylogenomics of Endogonales and evolution of mycorrhizas within Mucoromycota. *New Phytologist* 222(1): 511-525.

Chang Y, Wang Y, Mondo S, Ahrendt S, Andreopoulos W, Barry K, Beard J, Benny GL, Blankenship S, Bonito G et al. 2022. Evolution of zygomycete secretomes and the origins of terrestrial fungal ecologies. *iScience* 25(8): 104840.

Chen J, Tang Y, Kohler A, Lebreton A, Xing YM, Zhou D, Li Y, Martin FM, Guo S. 2022. Comparative transcriptomics analysis of the symbiotic germination of *D. officinale* (Orchidaceae) with emphasis on plant cell wall modification and cell wall-degrading enzymes. *Frontiers in Plant Science* 13:880600.

Chen M, Arato M, Borghi L, Nouri E, Reinhardt D. 2018. Beneficial services of arbuscular mycorrhizal fungi – from ecology to application. *Frontiers in Plant Science* 9: 1270.

Danecek P, Bonfield JK, Liddle J, Marshall J, Ohan V, Pollard MO, Whitwham A, Keane T, McCarthy SA, Davies RM, Li H. 2021. Twelve years of SAMtools and BCFtools. *GigaScience* 10(2): giab008.

De Castro E, Sigrist CJ, Gattiker A, Bulliard V, Langendijk-Genevaux PS, Gasteiger E, Bairoch A, Hulo N. 2006. ScanProsite: detection of PROSITE signature matches and ProRule-associated functional and structural residues in proteins. *Nucleic Acids Research* 34: 362-5.

Desirò A, Rimington WR, Jacob AS, Pol NV, Smith MR, Trappe JM, Bidartondo MI, Bonito G. 2017. Multigene phylogeny of Endogonales, an early diverging lineage of fungi associated with plants. *IMA Fungus* 8(2): 245–257.

Eddy SR. 2011. Accelerated profile HMM searches. *PLOS Computational Biology* 7(10): e1002195.

Frąc M, Hannula SE, Bełka M, Jędryczka M. 2018. Fungal biodiversity and their role in soil health. *Frontiers in Microbiology* 9: 707.

Gianinazzi-Pearson V, Morandi D, Dexheimer J, Gianinazzi S. 1981. Ultrastructural and ultracytochemical features of a *Glomus tenuis* mycorrhiza. *New Phytologist* 88(4): 633-639.

Gómez-Gallego T, Benabdellah K, Merlos MA, Jiménez-Jiménez AM, Alcon C, Berthomieu P, Ferrol N. 2019. The *Rhizophagus irregularis* genome encodes two CTR copper transporters that mediate Cu import into the cytosol and a CTR-like protein likely involved in copper tolerance. *Frontiers in Plant Science* 10: 604.

Gong Y, Lebreton A, Zhang F, Martin FM. 2023. Role of carbohydrate-active enzymes in mycorrhizal symbioses. *Essays in Biochemistry* 67(3): 471-478.

Gosling P, Mead A, Proctor M, Hammond JP, Bending GD. 2013. Contrasting arbuscular mycorrhizal communities colonizing different host plants show a similar response to a soil phosphorus concentration gradient. *New Phytologist* 198(2): 546-556.

Grigoriev IV, Nikitin R, Haridas S, Kuo A, Ohm R, Otillar R, Riley R, Salamov A, Zhao X, Korzeniewski F et al. 2013. MycoCosm portal: gearing up for 1000 fungal genomes. *Nucleic Acids Research* 42: 699-704.

Gruber-Vodicka HR, Seah BKB, Pruesse E. 2020. phyloFlash: Rapid small-subunit rRNA profiling and targeted assembly from metagenomes. m*Systems* 5(5): e00920-20.

Harrison MJ, Pumplin N, Breuillin FJ, Noar RD, Park HJ. 2010. Phosphate transporters in arbuscular mycorrhizal symbiosis. In: Koltai H, Kapulnik Y, eds. *Arbuscular Mycorrhizas: Physiology and Function.* Dordrecht, Netherlands: Springer, 117–135.

Hawkins HJ, Cargill RIM, Nuland MEV, Hagen SC, Field KJ, Sheldrake M, Soudzilovskaia NA, Kiers TE. 2023. Mycorrhizal mycelium as a global carbon pool. *Current Biology* 33(11): 560-573.

Hirose D, Degawa Y, Yamamoto K, Yamada A. 2014. Sphaerocreas pubescens is a member of the Mucoromycotina closely related to fungi associated with liverworts and hornworts. *Mycoscience* 55(3): 221-226.

Hoang DT, Chernomor O, von Haeseler A, Minh BQ, Vinh LS. 2018. UFBoot2: Improving the ultrafast bootstrap approximation. *Molecular Biology and Evolution*. 35: 518–522.

Horton P, Park KJ, Obayashi T, Fujita N, Harada H, Adams-Collier CJ, Nakai N. 2007. WoLF PSORT: protein localization predictor. *Nucleic Acids Research* 5(2): 585–587.

Howard NAO, Williams A, Durant E, Pressel S, Daniell TJ, Field KJ. 2024. Preferential nitrogen and carbon exchange dynamics in Mucoromycotina “fine root endophyte”-plant symbiosis. *Current Biology*.

Hoysted GA, Field KJ, Sinanaj B, Bell CA, Bidartondo MI, Pressel S. 2022. Direct nitrogen, phosphorus and carbon exchanges between Mucoromycotina ‘fine root endophyte’ fungi and a flowering plant in novel monoxenic cultures. *New Phytologist* 238(1): 70-79.

Hoysted GA, Jacob AS, Kowal J, Giesemann P, Bidartondo MI, Duckett JG, Gebauer G, Rimington WR, Schornack S, Pressel S et al. 2019. Mucoromycotina fine root endophyte fungi form nutritional mutualisms with vascular plants. *Plant Physiology* 181(2): 565-577.

Huey CJ, Gopinath SCB, Uda MNA, Zulhaimi HI, Jaafar MN, Kasim FH, Yaakub ARW. 2020. Mycorrhiza: a natural resource assists plant growth under varied soil conditions. *3Biotech* 10(5): 204.

Janusz G, Pawlik A, Sulej J, Świderska-Burek U, Jarosz-Wilkołazka A, Paszczyński A. 2017. Lignin degradation: microorganisms, enzymes involved, genomes analysis and evolution. *FEMS Microbiology Reviews* 41(6): 941-962.

Javot H, Pumplin N, Harrison MJ. 2006. Phosphate in the arbuscular mycorrhizal symbiosis: Transport properties and regulatory roles. *Plant, Cell & Environment* 30: 310–322.

Jeffery RP, Simpson RJ, Lambers H, Orchard S, Kidd DR, Haling RE, Ryan MH. 2018. Contrasting communities of arbuscule-forming root symbionts change external critical phosphorus requirements of some annual pasture legumes. *Applied Soil Ecology* 126: 88-97.

Kalyaanamoorthy S, Minh BQ, Wong TKF, von Haeseler A, Jermiin LS. 2017. ModelFinder: Fast model selection for accurate phylogenetic estimates. *Nature Methods.* 14: 587-589.

Katoh K, Standley DM. 2013. MAFFT multiple sequence alignment software version 7: improvements in performance and usability. *Molecular Biology and Evolution* 30(4): 772–780.

Kim GB, Kim JY, Lee JA, Norsigian CJ, Palsson BO, Lee SY. 2023. Functional annotation of enzyme-encoding genes using deep learning with transformer layers. *Nature Communications* 14: 7370.

Kobayashi Y, Maeda T, Yamaguchi K, Kameoka H, Tanaka S, Ezawa T, Shigenobu S, Kawaguchi M. 2018. The genome of Rhizophagus clarus HR1 reveals a common genetic basis for auxotrophy among arbuscular mycorrhizal fungi. *BMC Genomics* 19(1): 465.

Lanfranco L, Fiorilli V, Gutjahr C. 2018. Partner communication and role of nutrients in the arbuscular mycorrhizal symbiosis. *New Phytologist* 220(4): 1031-1046.

Lebreton A, Zeng Q, Miyauchi S, Kohler A, Dai YC, Martin FM. 2021. Evolution of the mode of nutrition in symbiotic and saprotrophic fungi in forest ecosystems. *Annual Review of Ecology, Evolution, and Systematics* 52(1): 385-404.

Lee S-J, Kong M, St-Arnaud M, Hijri M. 2020. Arbuscular mycorrhizal fungal communities of native plant species under high petroleum hydrocarbon contamination highlights Rhizophagus as a key tolerant genus. *Microorganisms* 8(6): 872.

Li H. 2013. Aligning sequence reads, clone sequences and assembly contigs with BWA-MEM. *ArXiv*. doi: 10.48550/arXiv.1303.3997

Liu A, Hamel C, Elmi A, Costa C, Ma B, Smith DL. 2002. Concentrations of K, Ca and Mg in maize colonized by arbuscular mycorrhizal fungi under field conditions. *Canadian Journal of Soil Science* 82(3): 271-279.

Luginbuehl LH, Menard GN, Kurup S, Van Erp H, Radhakrishnan GV, Breakspear A, Oldroyd GED, Eastmond PJ. 2017. Fatty acids in arbuscular mycorrhizal fungi are synthesized by the host plant. *Science* 365(6343): 1175-1178.

Luginbuehl LH, Oldroyd GED. 2017. Understanding the arbuscule at the heart of endomycorrhizal symbioses in plants. *Current Biology* 27(17): 952-963.

Maillard F, Schilling J, Andrews E, Schreiner KM, Kennedy P. 2020. Functional convergence in the decomposition of fungal necromass in soil and wood. *FEMS Microbiology Ecology* 96(2): fiz209.

Manni M, Berkeley MR, Seppey M, Simão FA, Zdobnov EM. 2021. BUSCO Update: Novel and streamlined workflows along with broader and deeper phylogenetic coverage for scoring of eukaryotic, prokaryotic, and viral genomes. *Molecular Biology and Evolution* 38(10): 4647-4654.

Mansfield TM, Albornoz FE, Ryan MH, Bending GD, Standish RJ. 2023. Niche differentiation of Mucoromycotinian and Glomeromycotinian arbuscular mycorrhizal fungi along a 2-million-year soil chronosequence. *Mycorrhiza* 33(3): 139-152.

Martin FM, van der Heijden MGA. 2024. The mycorrhizal symbiosis: research frontiers in genomics, ecology, and agricultural application. *New Phytologist* 242(4): 1486-1506.

Martino E, Morin E, Grelet G-A, Kuo A, Kohler A, Daghino S, Barry KW, Cichocki N, Clum A, Dockter RB et al. 2018. Comparative genomics and transcriptomics depict ericoid mycorrhizal fungi as versatile saprotrophs and plant mutualists. *New Phytologist* 217(3): 1213-1229.

McGonigle TP, Miller MH, Evans DG, Fairchild GL, Swan JA. 1990. A new method which gives an objective measure of colonization of roots by vesicular—arbuscular mycorrhizal fungi. *New Phytologist* 155(3): 495-501.

Minh BQ, Schmidt HA, Chernomor O, Schrempf D, Woodhams MD, von Haeseler A, Lanfear R. 2020. IQ-TREE 2: New models and efficient methods for phylogenetic inference in the genomic era. *Molecular Biology and Evolution*. 37(5): 1530-1534.

Mistry J, Bateman A, Finn RD. 2007. Predicting active site residue annotations in the Pfam database. *BMC Bioinformatics* 8: 298.

Miyauchi S, Kiss E, Kuo A, Drula E, Kohler A, Sánchez-García M, Morin E, Andreopoulos B, Barry KW, Bonito G et al. 2020. Large-scale genome sequencing of mycorrhizal fungi provides insights into the early evolution of symbiotic traits. *Nature Communications* 11: 5125.

Möller S, Croning MDR, Apweiler R. 2001. Evaluation of methods for the prediction of membrane spanning regions. *Bioinformatics* 17(7): 646–653.

Montoliu-Nerin M, Sánchez-García M, Bergin C, Kutschera VE, Johannesson H, Bever JD, Rosling A. 2021. In-depth phylogenomic analysis of arbuscular mycorrhizal fungi based on a comprehensive set of de novo genome assemblies. *Frontiers in Fungal Biology* 29(2): 716385.

Morin E, Miyauchi S, Clemente HS, Chen ECH, Pelin A, Providencia I, Ndikumana S, Beaudet D, Hainaut M, Drula E et al. 2019. Comparative genomics of *Rhizophagus irregularis* , *R. cerebriforme* , *R. diaphanus* and *Gigaspora rosea* highlights specific genetic features in Glomeromycotina. *New Phytologist* 222(3): 1584-1598.

Morris JL, Puttick MN, Clark JW, Edwards D, Kenrick P, Pressel S, Wellman CH, Yang Z, Schneider H, Donoghue PCJ. 2018. The timescale of early land plant evolution. *Proceedings of the National Academy of Sciences* 115(10): 2274-2283.

Naranjo-Ortiz MA, Gabaldón T. 2019. Fungal evolution: major ecological adaptations and evolutionary transitions. *Biological Reviews* 94(4): 1443–1476.

Öpik M, Davison J, Moora M, Zobel M. 2014. DNA-based detection and identification of Glomeromycota: the virtual taxonomy of environmental sequences. *Botany-Botanique* 92: 135–147.

Orchard S, Hilton S, Bending GD, Dickie IA, Standish RJ, Gleeson DB, Jeffery RP, Walker C, Bass D, Monk J et al. 2017a. Fine endophytes (Glomus tenue) are related to Mucoromycotina, not Glomeromycota. *New Phytologist* 213(2): 481-486.

Orchard S, Standish RJ, Dickie IA, Renton M, Walker C, Moot D, Ryan MH. 2017b. Fine root endophytes under scrutiny: a review of the literature on arbuscule-producing fungi recently suggested to belong to the Mucoromycotina. *Mycorrhiza* 27(7): 619-638.

Orchard S, Standish RJ, Nicol D, Gupta VVSR, Ryan MH. 2016. The response of fine root endophyte (Glomus tenue) to waterlogging is dependent on host plant species and soil type. *Plant and Soil* 403: 305-315.

Palos-Fernández R, Aguilar-Pontes MV, Puebla-Planas G, Berger H, Studt-Reinhold L, Strauss J, Di Pietro A, López-Berges MS. 2024. Copper acquisition is essential for plant colonization and virulence in a root-infecting vascular wilt fungus. *bioRxiv*. doi: 10.1101/2024.04.23.590778

Parniske, M. 2008. Arbuscular mycorrhiza: the mother of plant root endosymbiosis. *Nature Reviews Microbiology* 6: 763–775.

Peay KG, Kennedy PG, Talbot JM. 2016. Dimensions of biodiversity in the Earth mycobiome. *Nature Reviews Microbiology* 14: 434–447.

Pellegrin C, Morin E, Martin FM, Veneault-Fourrey C. 2015. Comparative analysis of secretomes from ectomycorrhizal fungi with an emphasis on small-secreted proteins. *Frontiers in Microbiology* 6: 1278.

Peng X, Wilken SE, Lankiewicz TS, Gilmore SP, Brown JL, Henske JK, Swift CL, Salamov A, Barry K, Grigoriev IV et al. 2021. Genomic and functional analyses of fungal and bacterial consortia that enable lignocellulose breakdown in goat gut microbiomes. *Nature Microbiology* 6: 499–511.

Petersen TN, Brunak S, von Heijne G, Nielsen H. 2011. SignalP 4.0: discriminating signal peptides from transmembrane regions. *Nature Methods* 8(10): 785-6.

Plassard C, Becquer A, Garcia, K. 2019. Phosphorus transport in mycorrhiza: How far are we?. *Trends in Plant Science* 24: 794–801.

Prout JN, Williams A, Wanke A, Schornack S, Ton J, Field KJ. 2024. Mucoromycotina 'fine root endophytes': a new molecular model for plant–fungal mutualisms?. *Trends in Plant Science* 29(6): 650-661.

Quast C, Pruesse E, Yilmaz P, Gerken J, Schweer T, Yarza P, Peplies J, Glöckner FO. 2013. The SILVA ribosomal RNA gene database project: improved data processing and web-based tools. *Nucleic Acids Research* 41: 590–596.

Quinlan AR, Hall IM. 2010. BEDTools: a flexible suite of utilities for comparing genomic features. *Bioinformatics* 26(6): 841-2.

R Core Team. 2023. R: A language and environment for statistical computing. R Foundation for Statistical Computing, Vienna, Austria. https://www.R-project.org/.

Rambaut, A. 2009. Figtree. Tree figure drawing tool, v1.4.4. Edinburgh, Scotland. http://tree.bio.ed.ac.uk/software/figtree.

Rasmussen HN, Rasmussen FN. 2014. Seedling mycorrhiza: a discussion of origin and evolution in Orchidaceae. *Botanical Journal of the Linnean Society* 175(3): 313-327.

Read DJ, Duckett JG, Francis R, Ligron R, Russell A. 2000. Symbiotic fungal associations in 'lower' land plants. *Philosophical Transactions of the Royal Society of London* 355(1398): 815–831.

Rimington WR, Pressel S, Duckett JG, Field KJ, Read DJ, Bidartondo MI. 2018. Ancient plants with ancient fungi: liverworts associate with early-diverging arbuscular mycorrhizal fungi. *Proceedings of the Royal Society B: Biological Sciences* 285(1888): 20181600.

Rosling A, Sahraei SE, Khan FK, Desirò A, Bryson AE, Mondo SJ, Grigoriev IV, Bonito G. Sánchez-García M. 2024. Evolutionary history of arbuscular mycorrhizal fungi and genomic signatures of obligate symbiosis. *BMC Genomics* 25: 529.

Ryan MH, McCully ME, Huang CX. 2003. Location and quantification of phosphorus and other elements in fully hydrated, soil-grown arbuscular mycorrhizas: a cryo-analytical scanning electron microscopy study. *New Phytologist* 160(2):429-441.

Sahu PK, Jayalakshmi K, Tilgam J, Gupta A, Nagaraju Y, Kumar A, Hamid S, Singh HV, Minkina T et al. 2022. ROS generated from biotic stress: Effects on plants and alleviation by endophytic microbes. *Frontiers in Plant Science* 13: 1042936.

Saier MH, Reddy VS, Moreno-Hagelsieb G, Hendargo KJ, Zhang Y, Iddamsetty V, Lam KJK, Tian N, Russum S, Wang J, Medrano-Soto A. 2021. The transporter classification database (TCDB): 2021 update. *Nucleic Acids Research* 49(1): 461-467.

Schüßler A, Martin H, Cohen D, Fitz M, Wipf D. 2007. Arbuscular mycorrhiza: studies on the geosiphon symbiosis lead to the characterization of the first glomeromycotan sugar transporter. *Plant Signaling & Behavior* 2(5), 431–434.

Schüßler A, Schwarzott D, Walker C. 2001. A new fungal phylum, the Glomeromycota: phylogeny and evolution. *Mycological Research* 105(12): 1413-1421.

Seeliger M, Hilton S, Muscatt G, Walker C, Bass D, Albornoz F, Standish RJ, Gray ND, Mercy L, Rempelos L et al. 2024. New fungal primers reveal the diversity of

Mucoromycotinian arbuscular mycorrhizal fungi and their response to nitrogen application. *Environmental Microbiome* 19: 71.

Setubal JC. 2021. Metagenome-assembled genomes: concepts, analogies, and challenges. *Biophysical Reviews* 13(6): 905–909.

Shen Z, Robert L, Stolpman M, Che Y, Allen KJ, Saffery R, Walsh A, Young A, Eckert J, Deming C et al. 2023. A genome catalog of the early-life human skin microbiome. *Genome Biology* 24(252).

Shi Z, Deng R, Yuan Q, Mao Z, Wang R, Li H, Liao X, Ma H. 2023. Enzyme commission number prediction and benchmarking with hierarchical dual-core multitask learning framework. *Research* 31(6): 0153

Singh NK, Wood JM, Patane J, Moura LMS, Lombardino J, Setubal JC, Venkateswaran K. 2023. Characterization of metagenome-assembled genomes from the International Space Station. Microbiome 11(1): 125.

Smith AD, Logeman BL, Thiele DJ. 2017. Copper acquisition and utilization in fungi. *Annual Review of Microbiology* 8(71): 597-623.

Spatafora JW, Chang Y, Benny GL, Lazarus K, Smith ME, Berbee ML, Bonito G, Corradi N, Grigoriev I, Gryganskyi A et al. 2016. A phylum-level phylogenetic classification of zygomycete fungi based on genome-scale data. *Mycologia* 108(5): 1028–1046.

Strullu-Derrien C, Selosse M-A, Kenrick P, Martin FM. 2018. The origin and evolution of mycorrhizal symbioses: from palaeomycology to phylogenomics. *New Phytologist* 220(4): 1012-1030.

Sujkowska-Rybkowska M, Znojek E. 2018. Localization of calreticulin and calcium ions in mycorrhizal roots of Medicago truncatula in response to aluminum stress. *Journal of Plant Physiology* 229: 22-31.

Tagirdzhanova G, Saary P, Tingley JP, Díaz-Escandón D, Abbott DW, Finn RD, Spribille T. 2021. Predicted input of uncultured fungal symbionts to a lichen symbiosis from metagenome-assembled genomes. *Genome Biology and Evolution* 13(4).

Talbot JM, Allison SD, Treseder KK. 2008. Decomposers in disguise: mycorrhizal fungi as regulators of soil C dynamics in ecosystems under global change. *Functional Ecology* 22(6): 955-963.

Tamura K, Stecher G, Kumar S. 2021. MEGA11: molecular evolutionary genetics analysis version 11. *Molecular Biology and Evolution* 38(7): 3022–3027.

Tanaka S, Hashimoto K, Kobayashi Y, Yano K, Maeda T, Kameoka H, Ezawa T, Saito K, Akiyama K, Kawaguchi M. 2022. Asymbiotic mass production of the arbuscular mycorrhizal fungus Rhizophagus clarus. *Communications Biology* 5: 43.

Tang N, Clemente HS, Roy S, Bécard G, Zhao B, Roux C. 2016. A survey of the gene repertoire of *Gigaspora rosea* unravels conserved features among Glomeromycota for obligate biotrophy. *Frontiers in Microbiology* 1(7):233.

Taylor A, Pereira N, Thomas B, Pink DAC, Jones JE, Bending GD. 2015. Growth and nutritional responses to arbuscular mycorrhizal fungi are dependent on onion genotype and fungal species. *Biology and Fertility of Soils* 51: 801–813.

Tedersoo L, Magurno F, Alkahtani S, Mikryukov V. 2024. Phylogenetic classification of arbuscular mycorrhizal fungi: new species and higher-ranking taxa in Glomeromycota and Mucoromycota (class Endogonomycetes). *MycoKeys* 107: 249-271.

Tedersoo L, Sánchez-Ramírez S, Kõljalg U, Bahram M, Döring M, Schigel D, May T, Ryberg M, Abarenkov K. 2018. High-level classification of the Fungi and a tool for evolutionary ecological analyses. *Fungal Diversity* 90: 135–159.

Thippayarugs S, Bansal M, Abbott LK. 1999. Morphology and infectivity of fine endophyte in a Mediterranean environment. *Mycological Research* 103(11): 1369-1379.

Tisserant E, Malbreil M, Kuo A, Kohler A, Symeonidi A, Balestrini R, Charron P, Duensing N, Frei dit Frey N, Gianinazzi-Pearson V et al. 2013. Genome of an arbuscular mycorrhizal fungus provides insight into the oldest plant symbiosis. *Proceedings of the National Academy of Sciences* 110(50):20117-20122.

Torres-Cruz TJ, Billingsley-Tobias TL, Almatruk M, Hesse CN, Kuske CR, Desirò A, Niccolò-Benucci GM, Bonito G, Stajich JE, Dunlap C et al. 2017. *Bifiguratus adelaidae*, gen. et sp. nov., a new member of Mucoromycotina in endophytic and soil-dwelling habitats. *Mycologia* 222(1): 511-525.

Vierheilig H, Coughlan AP, Wyss U, Piche Y. 1998. Ink and vinegar, a simple staining technique for arbuscular mycorrhizal fungi. *Applied and Environmental Microbiology* 64(12):5004-5007.

Vierstraete AR, Braeckman BP. 2022. Amplicon_sorter: A tool for reference-free amplicon sorting based on sequence similarity and for building consensus sequences. *Ecology and Evolution* 12(3): e8603.

Walker C, Gollotte A, Redecker D. 2018. A new genus, Planticonsortium (Mucoromycotina), and new combination (P. tenue), for the fine root endophyte, *Glomus tenue* (basionym *Rhizophagus tenuis*). *Mycorrhiza* 12(3): e8603.

Wang S, Zhang X, Zhang Z, Chen Y, Tian Q, Zeng D, Xu M, Wang Y, Dong S, Ma Z et al. 2023. Fusarium-produced vitamin B6 promotes the evasion of soybean resistance by *Phytophthora sojae*. *Journal of Integrative Plant Biology* 65(9): 2204-2217.

West PT, Probst AJ, Grigoriev IV, Thomas BC, Banfield JF. 2018. Genome-reconstruction for eukaryotes from complex natural microbial communities. *Genome Research* 28(4):569-580.

Wick RR, Schultz MB, Zobel J, Holt KE. 2015. Bandage: interactive visualisation of de novo genome assemblies. *Bioinformatics* 31(20): 3350-3352.

Wickham H. 2016. ggplot2: Elegant Graphics for Data Analysis. Springer-Verlag New York. ISBN 978-3-319-24277-4

Wurzbacher C, Larsson E, Johan Bengtsson-Palme, Van den Wyngaert S, Svantesson S, Kristiansson E, Kagami M, Nilsson HR. 2018. Introducing ribosomal tandem repeat barcoding for fungi. *Molecular Ecology Resources* 19(1):118-127.

Yamamoto K, Degawa Y, Yamada A. 2020. Taxonomic study of Endogonaceae in the Japanese islands: New species of *Endogone*, *Jimgerdemannia*, and *Vinositunica*, gen. nov.. *Mycologia* 112(2): 309-328.

Yang C, Chowdhury D, Zhang Z, Cheung WK, Lu A, Bian Z, Zhang L. 2021. A review of computational tools for generating metagenome-assembled genomes from metagenomic sequencing data. *Computational and Structural Biotechnology Journal* 19: 6301-6314.

Yu G, Smith DK, Zhu H, Guan Y, Lam TTY. 2017. ggtree: an r package for visualization and annotation of phylogenetic trees with their covariates and other associated data. *Methods in Ecology and Evolution* 8(1): 28-36.

Zhang H, Yohe T, Huang L, Entwistle S, Wu P, Yang Z, Busk PK, Xu Y, Yin Y. 2018. dbCAN2: a meta server for automated carbohydrate-active enzyme annotation. *Nucleic Acids Research* 46: 95-101.

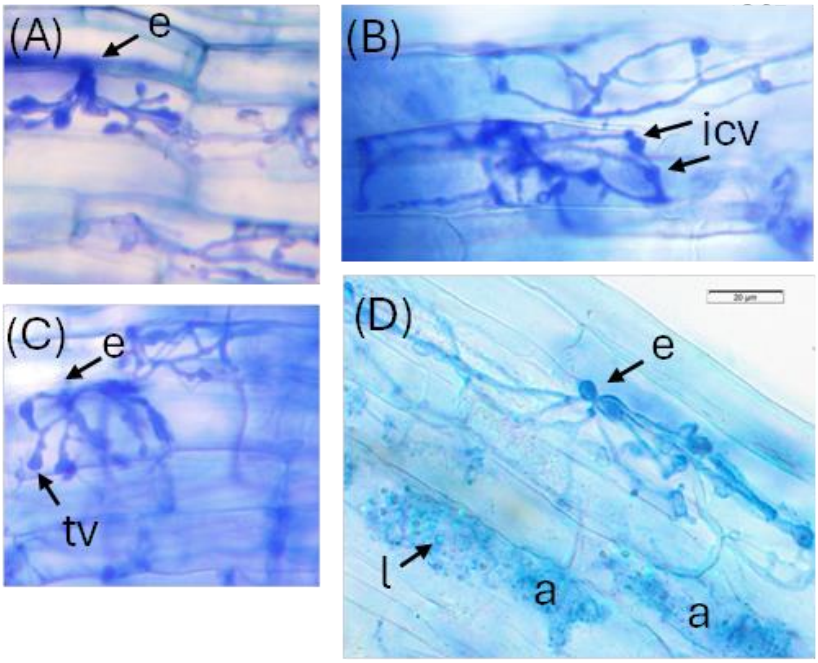

Figure 1. Colonisation by arbuscular mycorrhizal fungi (AMF) with fine root endophyte (FRE) morphology in the roots of *Trifolium subterraneum* from: (A, B, C) the experiment from which roots were chosen for metagenomic sequencing and (D) roots enriched in FRE which were used as the reference 18S rRNA sequence (FRE 4583) of Mucoromycotina-AMF (Orchard et al. (2017); experiment 1). Evident are the characteristic thin hyphae of FRE morphology, as well as entry points (e), several cells filled by an arbuscule (a) which also contained lipid droplets (l), terminal vesicles (tv) and intercalary vesicles (icv). (Photo credit: Payman Abbaszadeh-Dahaji A, B, C; Suzanne Orchard D)

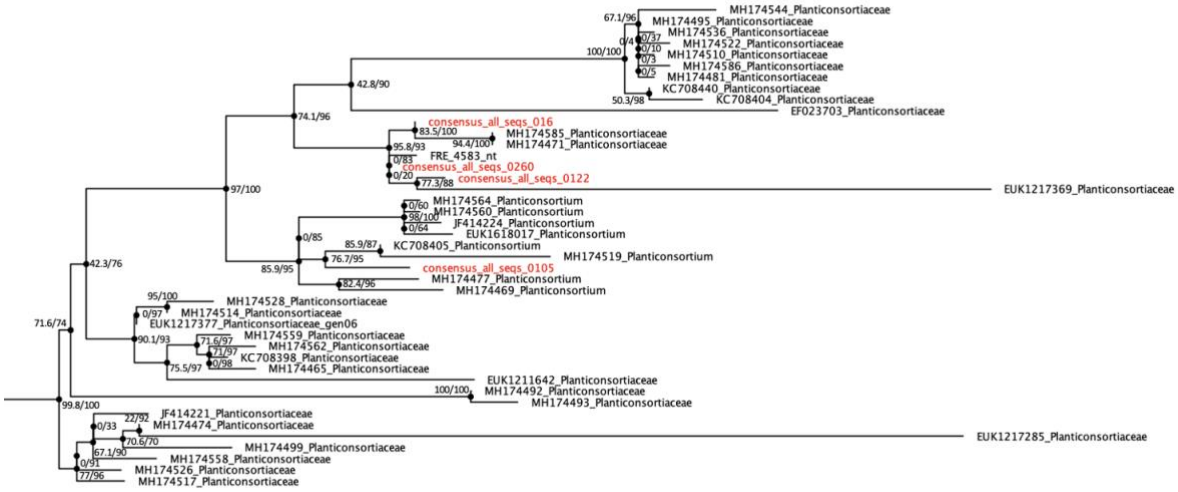

Figure 2. Phylogenetic assessment of the Mucoromycotina-AMF reference sequence FRE 4583 and ‘consensus_all_seqs_0_16’, an 18S rRNA gene sequence associated with the MAG, and related 18S rRNA sequences amplified from root samples (consensus_all_seqs_0122, 0105 and 0122), in the context of the Tedersoo et al. (2024) *Endogonomycetes* SSU alignment. The phylogenetic tree was generated using IQ-TREE, the model “TIM2+F+R5”, 1000 ultrafast bootstrap replicates, and approximate Likelihood Ratio Tests. Branch support is presented as a percentage (aLTR support/bootstrap support).

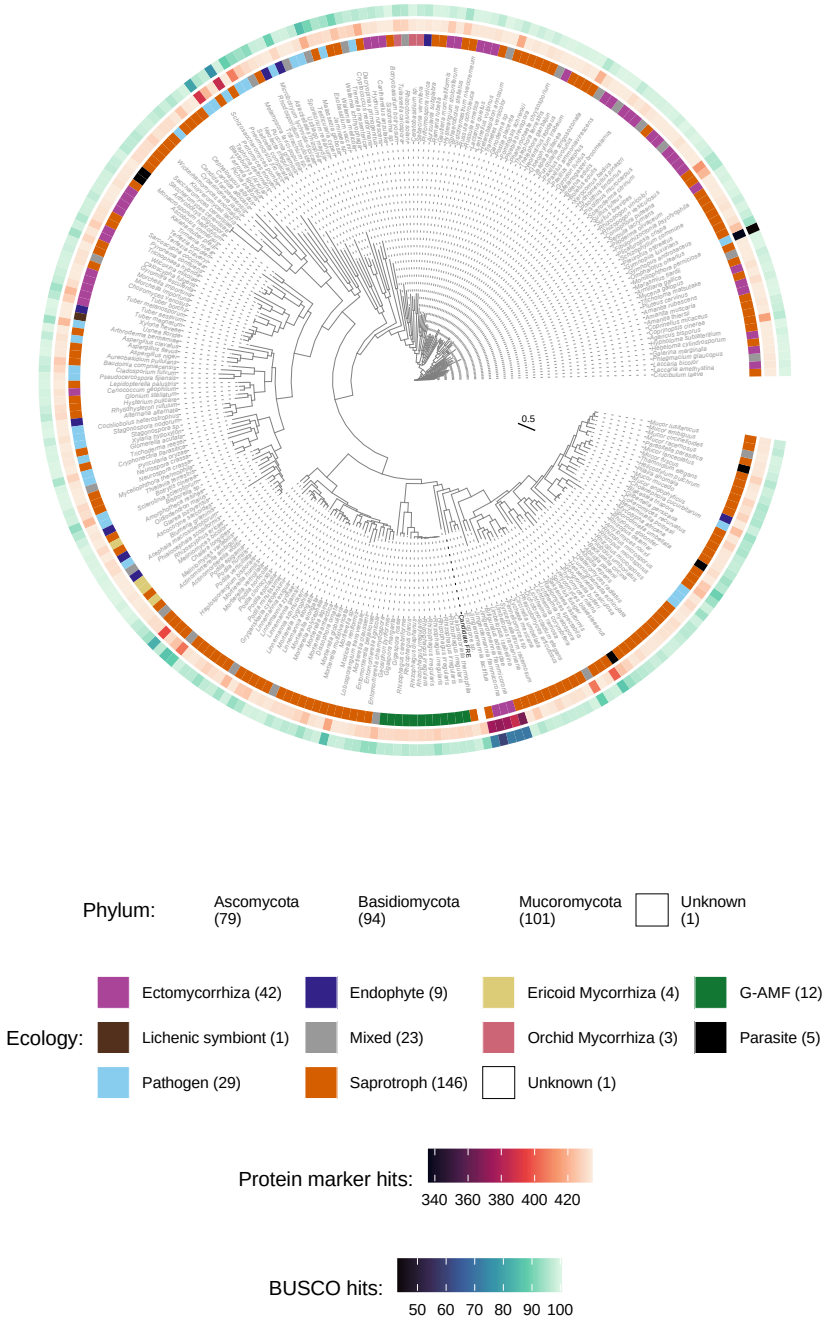

Figure 3. Phylogenetic placement of the MAG (Shown here as Candidate FRE) based upon a set of 434 protein markers identified by the JGI as pan-fungal markers for inferring high-level fungal phylogeny. Associated ecological group, protein marker hits and BUSCO hits are shown.

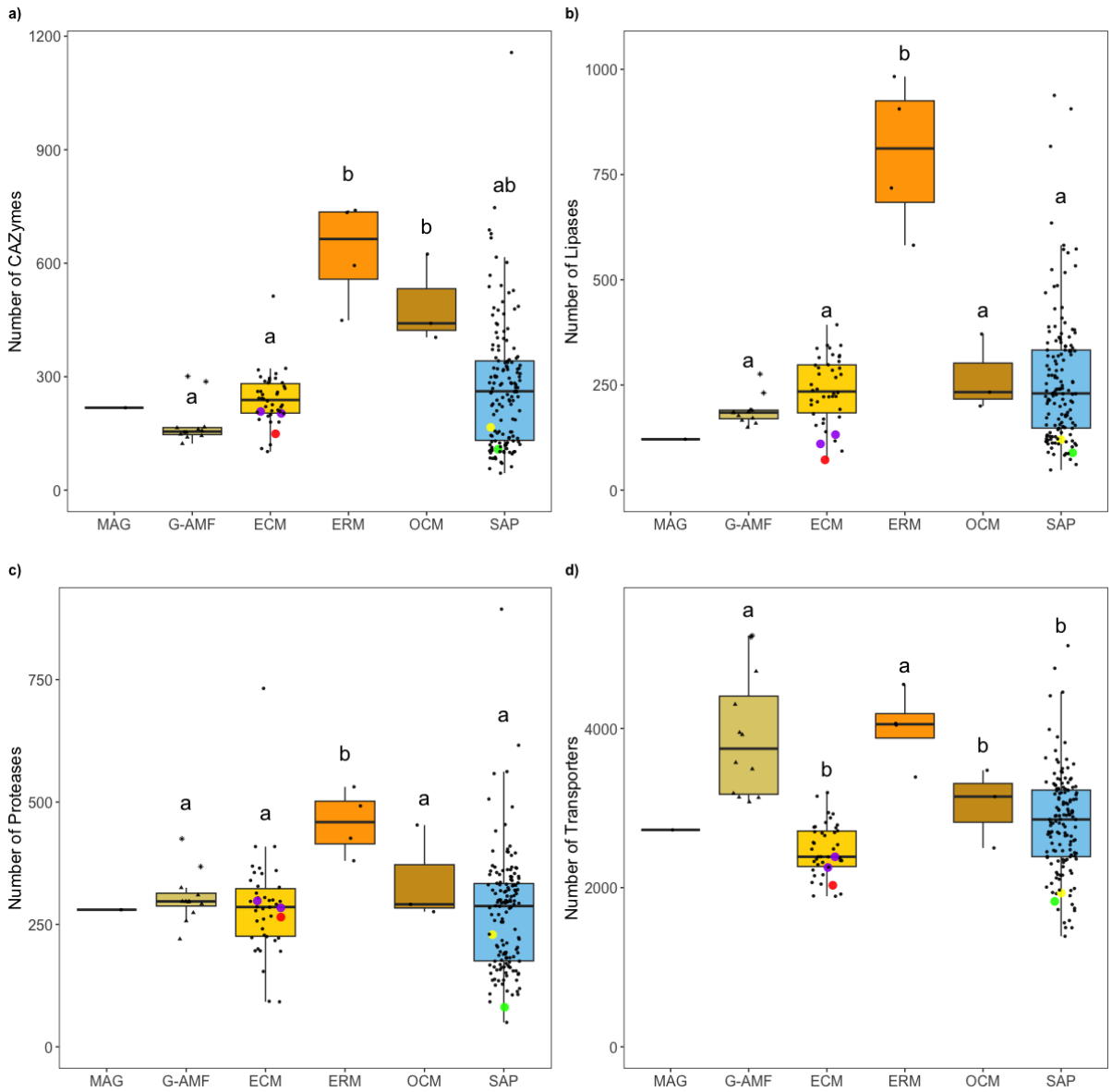

Figure 4. Number of CAZyme, lipase, protease, and transporter predicted proteins per genome distributed by ecological lifestyle. Lifestyle is colour coded. Coloured data points represent the phylogenetically closest relatives to the MAG: yellow for 'Endsp1', red for 'Jimlac1', green for 'Bifad1', and purple for both 'Jimfl_AD_1' and 'Jimfl_GMNB39_1'. Data point shape within the G-AMF distinguishes between the Diversisporales (star) and Glomerales (triangle). Different letters indicate significant differences between lifestyles as determined by a Kruskal-Wallis test ($p < 0.01$) followed by a post-hoc Dunn's test ($p < 0.05$).

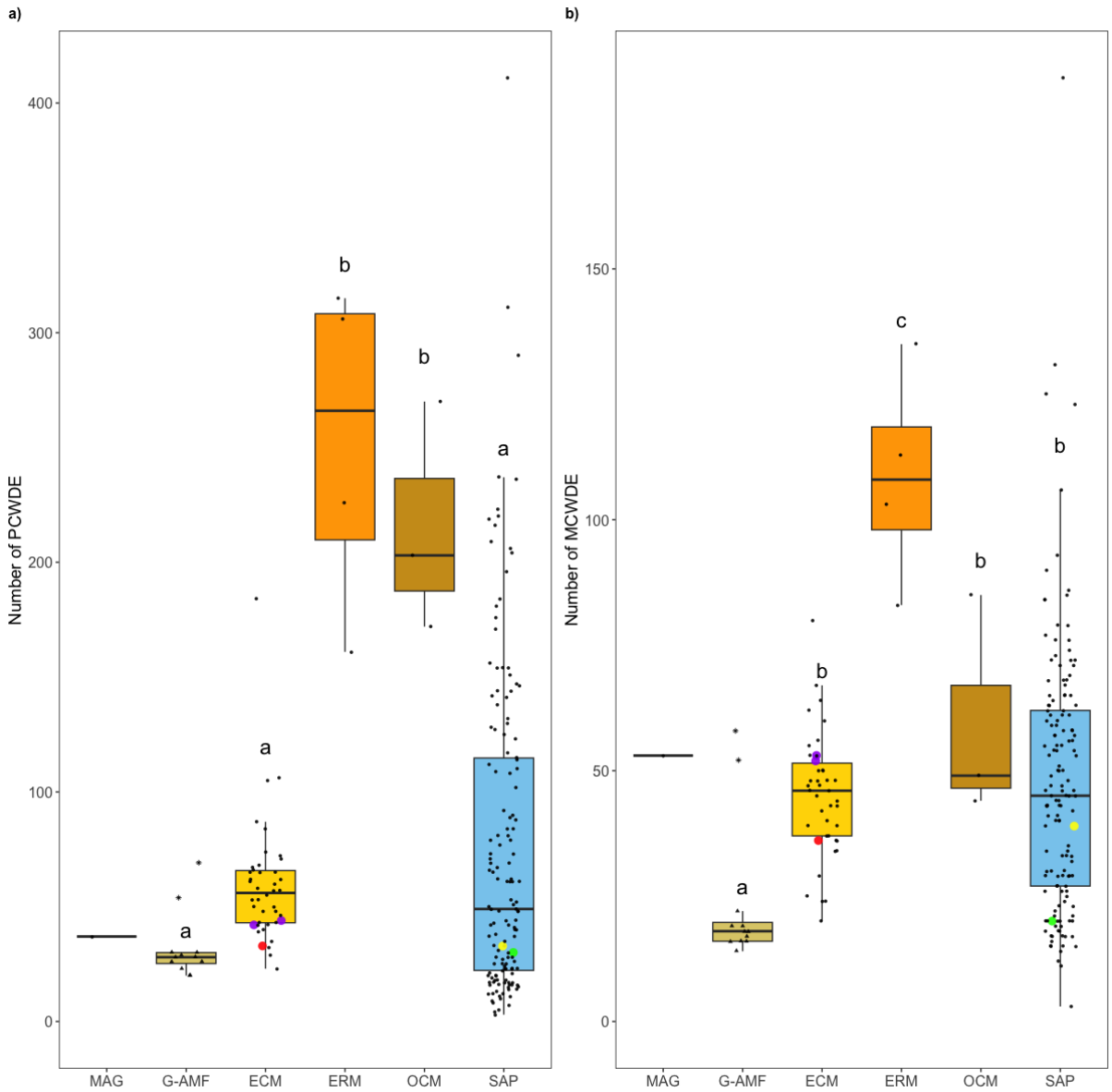

Figure 5. Number of plant cell wall degrading enzyme (PCWDE) and microbial cell wall degrading enzyme (MCWDE) predicted proteins per genome distributed by ecological lifestyle. Lifestyle is colour coded. Coloured data points represent the phylogenetically closest relatives to the MAG: yellow for 'Endsp1', red for 'Jimlac1', green for 'Bifad1', and purple for both 'Jimfl_AD_1' and 'Jimfl_GMNB39_1'. Data point shape within the G-AMF distinguishes between the Diversisporales (star) and Glomerales (triangle). Different letters indicate significant differences between lifestyles as determined by a Kruskal-Wallis test ($p < 0.01$) followed by a post-hoc Dunn's test ($p < 0.05$).

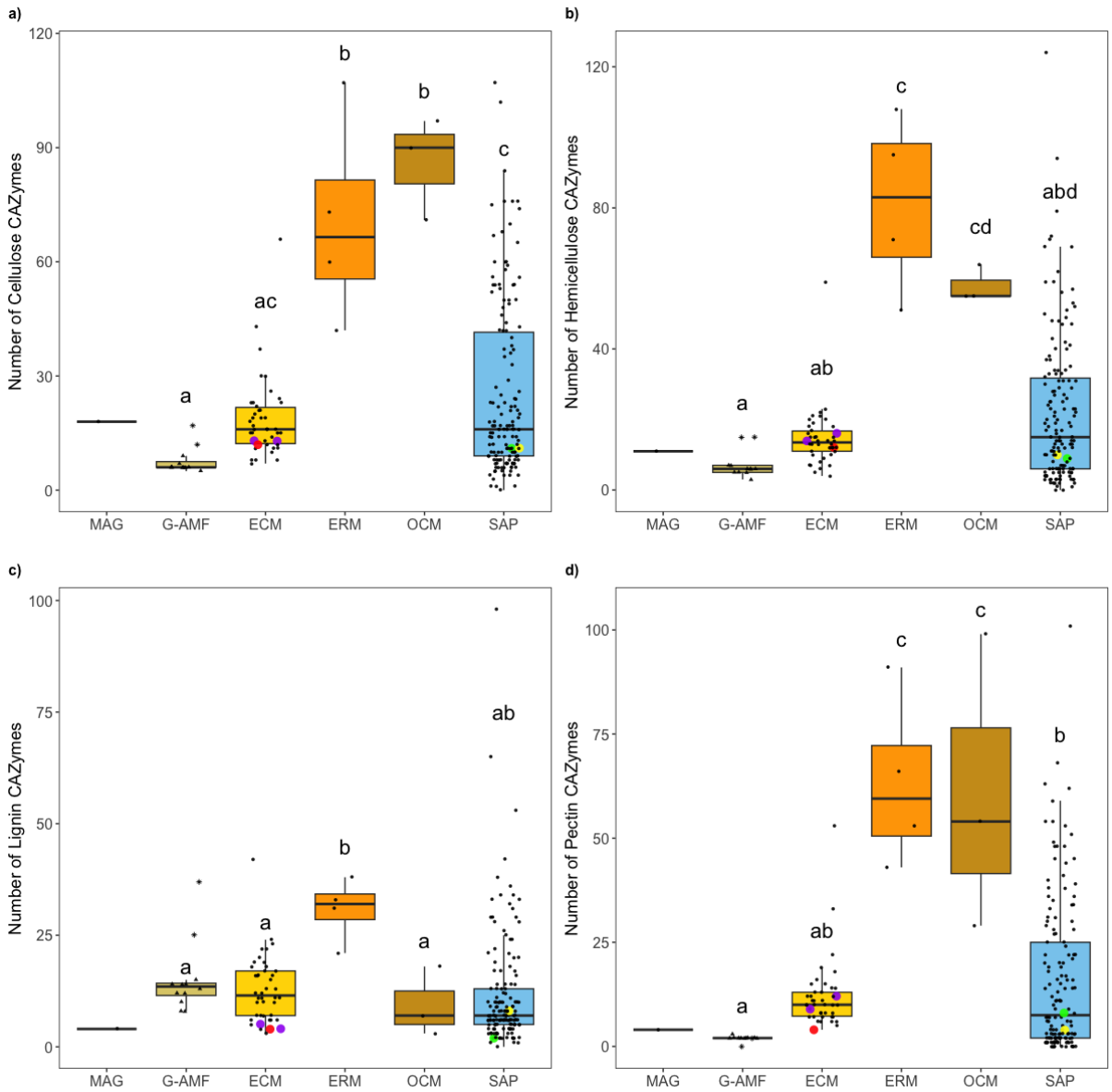

Figure 6. Cellulose, hemicellulose, lignin and pectin degrading predicted proteins per genome distributed by ecological lifestyle. Lifestyle is colour coded. Coloured data points represent the phylogenetically closest relatives to the FRE genome: yellow for ‘Endsp1’, red for ‘Jimlac1’, green for ‘Bifad1’, and purple for both ‘Jimfl_AD_1’ and ‘Jimfl_GMNB39_1’. Data point shape within the G-AMF distinguishes between the Diversisporales (star) and Glomerales (triangle). Different letters indicate significant differences between lifestyles as determined by a Kruskal-Wallis test ($p < 0.01$) followed by a post-hoc Dunn’s test ($p < 0.05$).

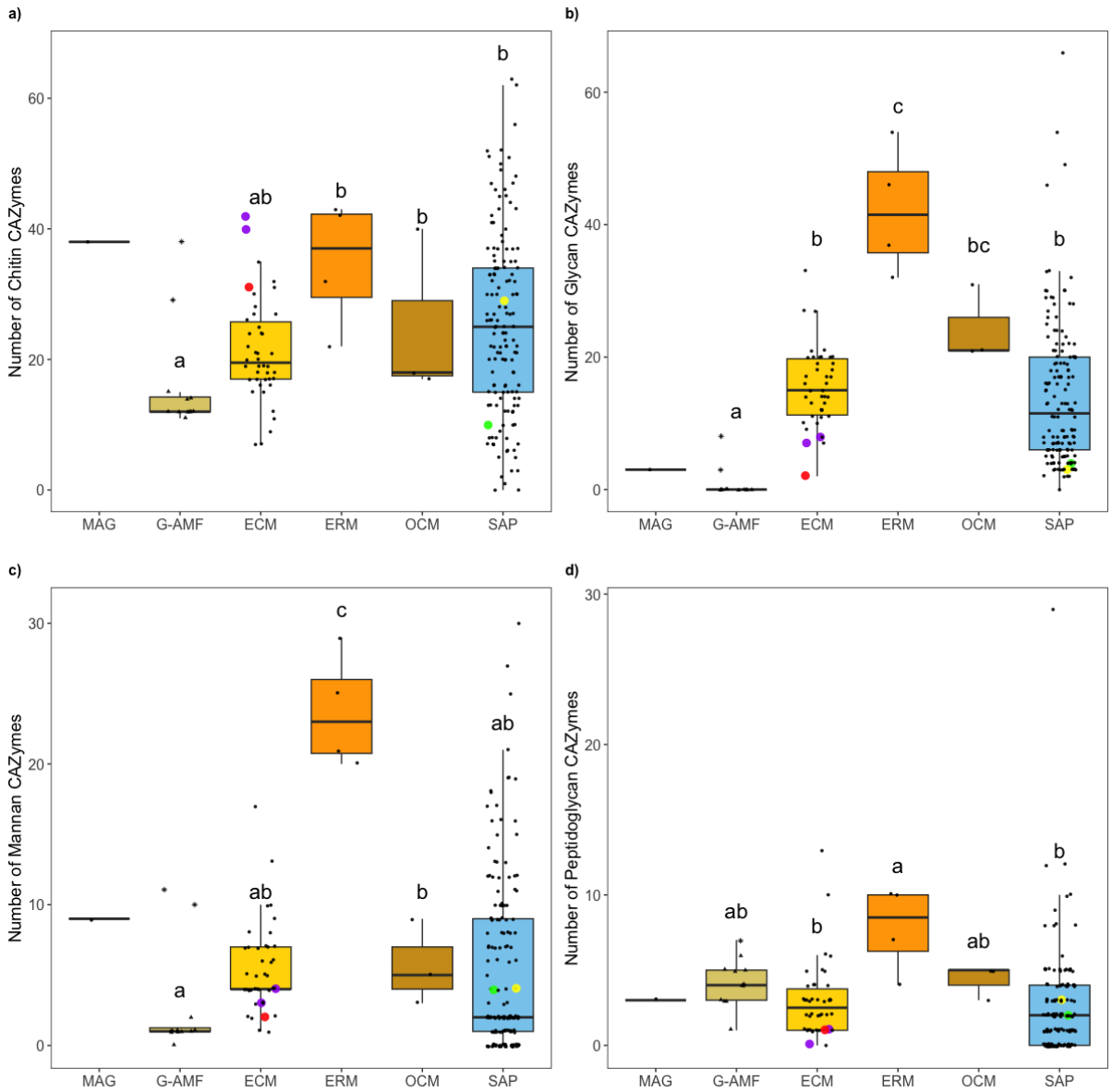

Figure 7. Chitin, glycan, mannan, and peptidoglycan degrading predicted proteins per genome distributed by ecological lifestyle. Lifestyle is colour coded. Coloured data points represent the phylogenetically closest relatives to the MAG: yellow for 'Endsp1', red for 'Jimlac1', green for 'Bifad1', and purple for both 'Jimfl_AD_1' and 'Jimfl_GMNB39_1'. Data point shape within the G-AMF distinguishes between the Diversisporales (star) and Glomerales (triangle). Different letters indicate significant differences between lifestyles as determined by a Kruskal-Wallis test ($p = 0.012$ for chitin, $p = 0.024$ for peptidoglycan, and $p < 0.01$ for the remainder) followed by a post-hoc Dunn's test ($p < 0.05$).

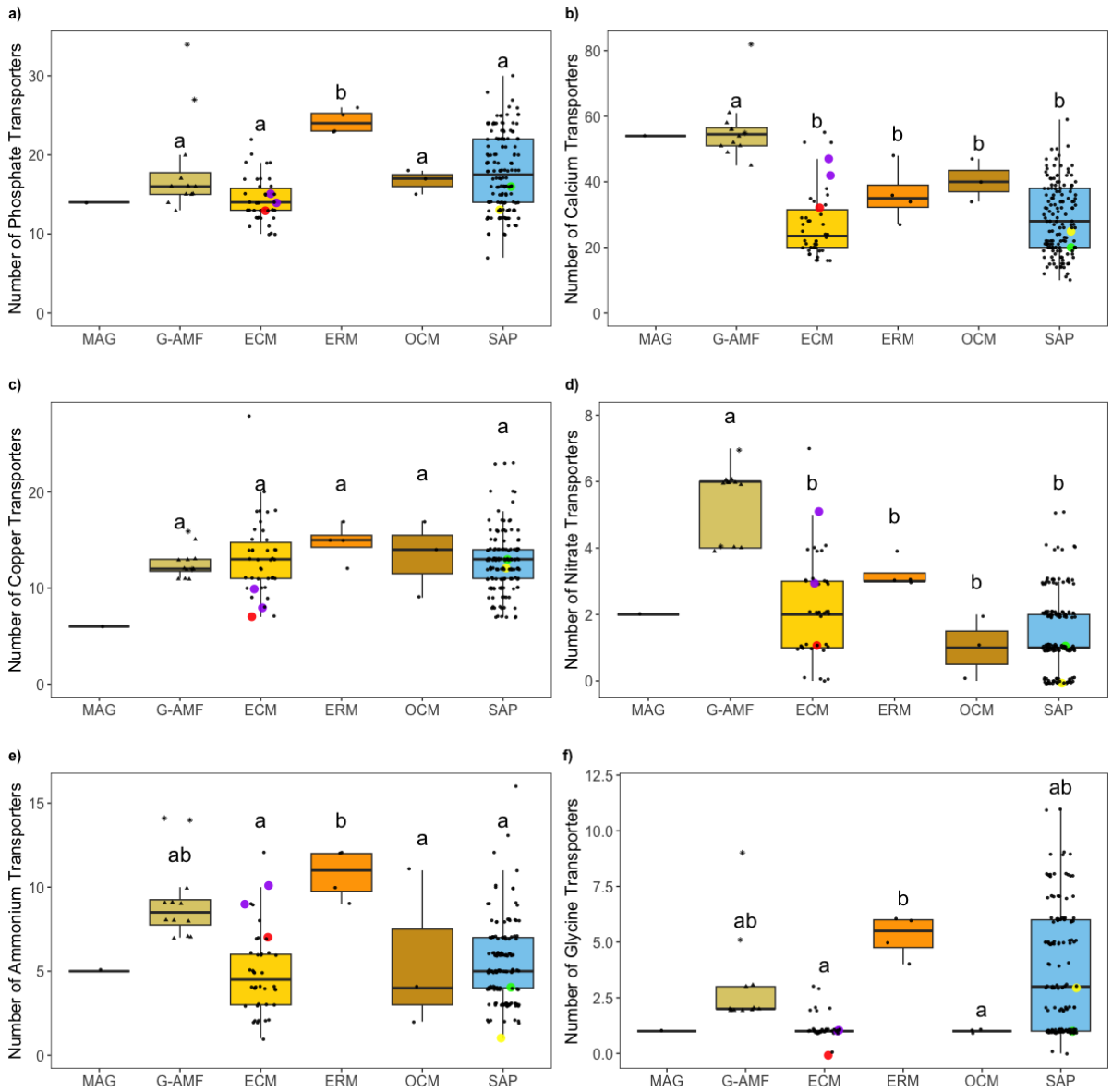

Figure 8: Phosphate, calcium, copper, nitrate, ammonium and glycine transporters per genome distributed by ecological lifestyle. Lifestyle is colour coded. Coloured data points represent the phylogenetically closest relatives to the MAG: yellow for ‘Endsp1’, red for ‘Jimlac1’, green for ‘Bifad1’, and purple for both ‘Jimfl_AD_1’ and ‘Jimfl_GMNB39_1’. Data point shape within the G-AMF distinguishes between the Diversisporales (star) and Glomerales (triangle). Different letters indicate significant differences between lifestyles as determined by a Kruskal-Wallis test ($p = 0.028$ for phosphate, $p = 0.62$ for copper, $p = 0.041$ for nitrate, and $p < 0.01$ for the remainder) followed by a post-hoc Dunn’s test ($p < 0.05$).